Agricultural and Forest Meteorology 307 (2021) 108521

Contents lists available at ScienceDirect

Agricultural and Forest Meteorology

journal homepage: www.elsevier.com/locate/agrformet

# Quantifying carbon budget, crop yields and their responses to environmental variability using the *ecosys* model for U.S. Midwestern agroecosystems

Wang Zhou[a,b,*], Kaiyu Guan[a,b,c,*], Bin Peng[a,b,c,*], Jinyun Tang[d], Zhenong Jin[e], Chongya Jiang[a,b], Robert Grant[f], Symon Mezbahuddin[f,g]

[a] Agroecosystem Sustainability Center, Institute for Sustainability, Energy, and Environment, University of Illinois at Urbana-Champaign, Urbana, IL 61801, USA
[b] Department of Natural Resources and Environmental Sciences, College of Agricultural, Consumer and Environmental Sciences, University of Illinois at Urbana-Champaign, Urbana, IL 61801, USA
[c] National Center for Supercomputing Applications, University of Illinois at Urbana-Champaign, Urbana, IL 61801, USA
[d] Earth and Environmental Sciences Area, Lawrence Berkeley National Laboratory, Berkeley, CA 94720, USA
[e] Department of Bioproducts and Biosystems Engineering, University of Minnesota, St. Paul, MN 55108, USA
[f] Department of Renewable Resources, University of Alberta, Edmonton, AB T6G2E3, Canada
[g] Natural Resource Management Branch, Alberta Agriculture and Forestry, Edmonton, AB, Canada

ARTICLE INFO

*Keywords:*
Carbon fluxes
Crop yield
*Ecosys*
Agroecosystems
Environmental variabilities
U.S. Midwest

ABSTRACT

As one of the major agricultural production areas in the world, the United States (U.S.) Midwest plays a vital role in the global food supply and agricultural ecosystem services. Although significant efforts have been made in modeling the carbon cycle dynamics over this area, large uncertainty still exists in the previous simulations in terms of reproducing individual components of the carbon cycle and their responses to environmental variability. Here we evaluated the performance of an advanced agroecosystem model, *ecosys*, in simulating carbon budgets over the U.S. Midwest, considering both the magnitude of carbon flux/yield and its response to environmental (climate and soil) variability. We conducted model simulations and evaluations at 7 cropland eddy-covariance sites as well as over 293 counties of Illinois, Indiana, and Iowa in the U.S. Midwest. The site-level simulations showed that *ecosys* captured both the magnitude and seasonal patterns of carbon fluxes (i.e., net ecosystem carbon exchange (NEE), ecosystem gross primary production (GPP), and ecosystem respiration (Reco)), leaf area index (LAI), and dynamic plant carbon allocation processes, with $R^2$ equal to 0.92, 0.87, 0.87, and 0.78 for GPP, NEE, Reco, and LAI, respectively across all the sites compared with the observations. For regional scale simulations, *ecosys* reproduced the spatial distribution and interannual variability of corn and soybean yields with the constraints of observed yields and a new remotely sensed GPP product, with $R^2$ of multi-year averaged simulated and observed yield equal 0.83 and 0.80 for corn and soybean, respectively. The simulated responses of carbon cycle dynamics to environmental variability were consistent with that from the empirical observations at both site and regional scales. Our results demonstrated the applicability of *ecosys* in simulating the carbon cycle and soil carbon dynamics of the U.S. Midwestern agroecosystems under different climate and soil conditions.

## 1. Introduction

The terrestrial carbon balance of agroecosystems plays an important role in global carbon cycle (Dold et al., 2017; Verma et al., 2005). Depending on the temporal and spatial scales used for accounting as well as the geographical regions, croplands can be either carbon sinks or sources for the atmospheric $CO_2$ (Blanco-Canqui and Lal, 2004; Kimble et al., 1998). In the U.S. Midwest, about 30–50% of soil organic carbon (SOC) has been lost when compared with that before cultivation for most croplands (Lal, 2002). Since SOC content is often positively related to soil fertility, SOC loss may enhance crop yield loss risk under future climate conditions (Lal, 2011, 2004, 2001). Fortunately, with recommended management practices (RMPs, i.e., conservation tillage, cover crops, and biosolids and manure, etc.), prior studies show that U.S.

* Corresponding authors.
*E-mail addresses:* wangzhou@illinois.edu (W. Zhou), kaiyug@illinois.edu (K. Guan), binpeng@illinois.edu (B. Peng).

https://doi.org/10.1016/j.agrformet.2021.108521
Received 21 November 2020; Received in revised form 17 May 2021; Accepted 14 June 2021
Available online 19 July 2021
0168-1923/

croplands have the potential to sequester about 75-208 Tg C/year, which may recover 50–70% of the depleted soil carbon (Jarecki and Lal, 2003; Lal, 2011, 2007, 2002; Meena et al., 2020; Hutchinson et al., 2007; Chambers et al., 2016). Hence, in order to help realize this carbon sequestration potential in U.S. croplands and meanwhile ensure global food security, it is critical to accurately quantify the carbon balance of agroecosystems, including carbon fixation and emission.

The carbon inventory (West et al., 2013, 2010, 2008; West and Marland, 2002), derived from crop yield survey reports (Vogel, 2018), SOC measurements (van Wesemael et al., 2010), and observation-based gross primary production (GPP) estimations (Jiang et al., 2021), can provide several components of cropland carbon budget. Among these carbon inventory methods, soil-sampling-based SOC measurement is the most direct approach to investigate SOC change, but it still has uncertainties associated with soil sampling strategies (i.e., sampling location, depth, and time), measurement methods, and duration between measurements (Jandl et al., 2014; Schrumpf et al., 2011; VandenBygaart and Angers, 2006). More importantly, it is difficult to scale up the soil sampling due to its high labor and financial costs. In the framework of carbon balance, SOC change can in principle be derived from the whole carbon mass balance, which requires different carbon cycling components (i.e., GPP, ecosystem respiration (Reco), and harvest etc.). However, most of the carbon inventories cover only part of the carbon cycling components, such as agroecosystem carbon input (i.e., GPP) or outputs (i.e., yield). Measurements of other key carbon cycling components (i.e., respiration and litterfall) of agroecosystems are still difficult and insufficient, especially at large scales (e.g., U.S. Midwest) (Osborne et al., 2010). All these factors limit wide and robust applications of carbon inventory to quantify agroecosystem carbon budgets and SOC change.

Alternatively, we can use process-based models to quantify the cropland carbon budget (Brilli et al., 2017; Huang et al., 2009; Wattenbach et al., 2010; Zhang et al., 2015). However, existing studies using process-based models for cropland carbon budget quantification have suffered from one or few of the following limitations. First, very few model-based quantifications of the cropland carbon budget have gone through rigorous model validation covering the whole agroecosystem carbon cycle (i.e., carbon fixation, carbon allocation, and respiration), especially at regional scales. Most process-based modeling studies for agroecosystems evaluated and constrained their models with a limited number of observational variables, such as crop yield (Gilhespy et al., 2014; Stehfest et al., 2007) and/or measured SOC (Li et al., 1997; Liu et al., 2006; Shirato, 2005). This lack of sufficient model constraint may cause simulations to be apparently right with wrong reasons (Peng et al., 2018). For example, models can generate the same crop yield with higher carbon fixation but lower harvest index compared to the correct ones, because errors in plant carbon fixation can be reconciled by unconstrained fluxes of respiration and litterfall. Therefore, to ensure that the model simulates carbon emission and sequestration correctly in both short and long terms, we need to use more carbon-related observations with fine temporal resolution (i.e., daily GPP, net ecosystem carbon exchange (NEE), Reco, leaf area index (LAI), plant carbon allocation, and phenology) to sufficiently constrain and validate the carbon cycling processes of the models.

Second, most existing model-based studies only calibrated and validated the models at a few specific sites due to limited availability of observations. In general, models involve both parameters that are site-specific (i.e., maturity group and climate zone) and parameters that are shared among sites at a regional scale (i.e., parameters controlling the temperature responses of activity of RuBP carboxylase-oxygenase) (Kuppel et al., 2012; Mäkelä et al., 2007). Thus optimizing a model at specific sites will tie the resultant model parameterization closely to the site information (e.g., climate, soil, groundwater depth, field microtopography, and land management practices etc.), so that the model may not be suitable for other sites and regions with different soil and climate conditions. To ensure the model parameterization can be robustly transferred to other sites or regions, systematic evaluations are needed. Specifically, we need to constrain and evaluate models under a wide range of soil and climate conditions, using diverse data such as large-scale carbon inventories (e.g., crop yield reports and crop progress reports) and satellite remote sensing carbon-related observations (e.g., GPP and LAI).

Finally, current model calibrations and validations have generally focused on matching the magnitude or time series of the target variables (e.g., GPP and yield) (Gurung et. al., 2020; Wang et al., 2020; Jin et al., 2017), which is achieved by minimizing a cost function (which measures model-data discrepancy) that does not take into account the relationship between these target variables and environmental drivers. From the perspective of Bayesian inference (Tarantola, 2013), since only uncertainties in model parameters are constrained, such a practice leads to an underestimation of the prior information associated with the environmental drivers. To make a more comprehensive use of the information contained in observations and model driving variables, as well as to deliver more confident predictions of how agroecosystems will respond to environment changes, we thus further need to verify relationships between environment variables and model predicted variables to test whether the model can simulate emergent responses of those variables to environmental factors from empirical observations (Peng et al., 2020). The accurate representation of the response of the target variables to environmental factors (i.e., climate variability and soil conditions) will help expand the models to broader soil and climate conditions.

Based on the above rationales, to demonstrate a new standard to achieve a comprehensive constraint and evaluation of an agroecosystem simulator, in this study we used an advanced ecosystem model, *ecosys*, to simulate surface carbon fluxes and corn/soybean yield in the U.S. Midwest at both eddy-covariance sites and county scales for the three I states (Illinois, Iowa and Indiana). As one of the world's largest crop production areas, the U.S. Midwest produces about 85% of U.S. corn and soybean (USDA, 2020). The soil health and crop yield of the U.S. Midwest in the future is vital to the global food supply and agricultural ecosystem services. To improve the quantification of carbon cycle dynamics in the U.S. Midwest, both the absolute values of the simulated carbon fluxes and yield as well as the responses of those variables to the environmental variabilities were evaluated. Through the evaluations, we aim to evaluate the capability of *ecosys* in conducting spatiotemporal extrapolations of agroecosystem carbon cycle by addressing the following two questions: (1) To what extent can *ecosys* simulate agroecosystem carbon dynamics at different individual sites as well as across the broader regions in the U.S. Midwest? (2) How well can *ecosys* capture the responses of carbon fluxes and crop yield to environmental variabilities? Although we use *ecosys* as an example, the procedures for model evaluation described in this study are applicable to many other agroecosystem models.

## 2. Data and method

### 2.1. The process-based model ecosys

*Ecosys* is an advanced mechanistic ecosystem model developed to simulate water, energy, carbon, and nutrient cycles simultaneously for various ecosystems, including agroecosystems at hourly step (Fig. 1a) (Grant, 2001). It is one of the very few models that are formulated primarily based on biophysical and biochemical principles, with fully connected balances and interactions for water, energy, carbon and nutrient cycles in the soil-plant-atmosphere continuum, and has been extensively validated in various ecosystems ranging from agricultural (Grant et al., 2007, 2011; Mezbahuddin et al., 2020) to forest systems (Grant et al., 2001, 2010, R. F. Grant et al., 2006; R. Grant et al., 2006).

The *ecosys* model was built based on the strategy that pursues the mechanistic representations and model outputs as directly comparable to observations as possible to realistically inform agricultural practices,

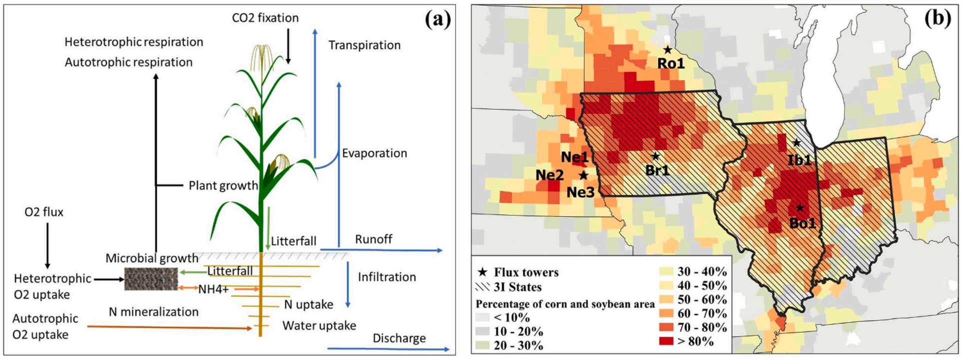


**Fig. 1.** (a) Major processes represented in the *ecosys* model (revised from (Grant, 2004)), and (b) locations of the seven eddy-covariance sites and the three I states in the U.S. Midwest.

by combining reactive transport modeling and state of the art knowledge of biogeochemistry (Grant, 2001). For example, photosynthesis and plant hydraulics in *ecosys* are coupled through leaf osmotic pressure, and then turgor pressure and leaf water potential that is linked to stomatal conductance (Grant, 1995; Grant and Flanagan, 2007), rather than empirical stress functions (Van den Hoof et al., 2011; Liu et al., 2016; Yokohata et al., 2020), and all of which can be measured in the field (Salmon et al., 2020; Shekoofa et al., 2021; Xue et al., 2021). As it integrates the plant hydraulics closely with the plant photosynthesis (Grant et al., 1999), the plant stomata conductance in *ecosys* is directly controlled by the balance between photosynthetic carbon assimilation and plant water hydraulics calculated for the soil-plant-atmosphere continuum, which can properly resolve the plant response to drought (Mekonnen et al., 2017). Due to the explicit simulation of plant hydraulic impacts on stomatal conductance, the empirical crop response to atmospheric vapor pressure deficit does not need be prescribed as in many other models (Van den Hoof et al., 2011; Liu et al., 2016; Yokohata et al., 2020). In response to soil water and plant carbon stress, *ecosys* also dynamically adjusts the plants' carbon and nutrient allocation strategies (Grant et al., 2001a), so that all plant organs will balance their respective growth to help the plants survive the harsh growth conditions and flourish under favorable conditions. In addition, the plant carbon and nutrient allocation is represented following the source-storage-sink balance approach, rather than the fixed allometric relationship approach adopted by most existing models (Grant, 1989b; Drewniak et al., 2013; Liu et al., 2016).

Moreover, *ecosys* employs much more complete physical and chemistry theories in simulating soil related processes. Specifically, *ecosys* mechanistically resolves the oxygen stress throughout the soil and plant roots (Grant, 1998), such that a flood condition will suppress plants' growth and alter the soil carbon and nutrient cycling. In addition, *ecosys* explicitly includes microbes' competitive and symbiotic nutrient interactions with plants (Grant and Pattey, 2003; Grant et al., 2006; Grant and Pattey, 2008; Grant et al., 2016), enabling a nutrient-based analysis of how various management practices can affect plant productivity. Meanwhile, soil organic carbon dynamics in *ecosys* are driven explicitly by microbial community dynamics that emerge from the interactions between bacteria and fungi, and another five functional groups carrying out fermentation, methane and nitrogen cycling (Grant, 2013; Grant and Rochette, 1994). Emergent microbial population structure, e.g., bacteria to fungi ratio, can be directly evaluated with respect to field measurements (Anderson and Domsch, 1975; Bardgett and McAlister, 1999). Moreover, the partitioning of soil carbon in *ecosys* is amenable to the density fractionation that is often used by empiricists to characterize soil organic matter. In addition, *ecosys* outputs profiles and fluxes of many easily measurable chemicals, including different phase existences of $CO_2$, $CH_4$, $N_2O$, $NH_3$, $NO_3$, $HPO_4^{(2-)}$, etc. Finally, *ecosys* resolves many common agricultural practices, such as mixed cropping, depth dependent irrigation and tillage (Grant, 1997), banded vs broadcast fertilization (Grant et al., 2001b), soil liming, manure application (Grant et al., 2001c), denitrification inhibitor (Grant et al., 2020), and tile-drainage system (Mezbahuddin et al., 2017) etc. Finally, *ecosys* generally requires no calibration for the soil and hydrological processes due to its complete mechanistics thus provides scalability to regional scale applications (Grant et al., 2012). All these features make *ecosys* stand out as an unique simulator as compared to many other models that tend to lump processes into simplified representations. We here refer detailed information about the processes represented in *ecosys* to the supplement of Grant et al. (2019), and the code of *ecosys* can be obtained from the online repository (https://github.com/jinyun1tang/ECOSYS). Below we only describe major carbon cycling processes of agro-ecosystems simulated in *ecosys* (Eqs. (1) and ((2)).

$$\begin{aligned} -\mathrm{NEE} &= \mathrm{GPP} - \mathrm{Reco} \\ &= \mathrm{GPP} - (\mathrm{Ra} + \mathrm{Rh}) \\ &= \mathrm{GPP} - ((\mathrm{Rm} + \mathrm{Rg}) + \mathrm{Rh}) \end{aligned} \tag{1}$$

$$\mathrm{NBP} = -\mathrm{NEE} - \mathrm{Yield} - \varepsilon \tag{2}$$

where NEE is net ecosystem exchange, GPP is gross primary production, Ra is ecosystem autotrophic respiration, Rh is ecosystem heterotrophic respiration, Reco is ecosystem respiration, Rm and Rg are plant maintenance and growth respiration, NBP is net biome productivity, Yield is harvested crop yield, and $\varepsilon$ is the carbon losses caused by disturbances (e.g., fire) excluding harvest.

In *ecosys*, the change of SOC ($\Delta$SOC) is equal to the difference between plant litter fall, Rh, and ecosystem carbon leakage, including $CH_4$ emission, dissolved organic (DOC) and inorganic carbon (DIC) leaching, etc (Eq. (3a)). For annual cropping system in most of the U.S. Corn Belt regions, we can use NBP to approximate $\Delta$SOC at long term scales ($\geq$annual scale). By using Eq. 3, most part of simulated cropland soil carbon balance can be directly backuped with the eddy-covariance measurements or carbon inventory data, which provided another approach to evaluate and verify the model performance in carbon budget estimations (Baker and Griffis, 2005).

$$\Delta \mathrm{SOC} = \mathrm{Litter\_Fall} - \mathrm{Rh} - \varepsilon \tag{3a}$$

$$= (\mathrm{GPP} - \mathrm{Ra} - \mathrm{Yield} + \mathrm{Seed\_C}) - \mathrm{Rh} - \varepsilon \tag{3b}$$

$$= -\mathrm{NEE} + \mathrm{Seed\_C} - \mathrm{Yield} - \varepsilon \tag{3c}$$

$$\begin{aligned} &= \mathrm{NBP} + \mathrm{Seed\_C} - \varepsilon \\ &\text{(3b)-(3d) works} \geq \text{annual scale for annual cropping systems} \end{aligned} \tag{3d}$$

where Litter_Fall is the litter fall from plants, including leaf senescence, harvest residue, and root carbon exudation, Seed_C is the seed mass at planting, $\varepsilon$ is the carbon leakage through $CH_4$ emission, and DOC and DIC are leaching terms.

### 2.1.1. Photosynthesis (GPP)

The *ecosys* model uses a multiple-layer canopy module to simulate canopy light absorption and carbon assimilation (Grant et al., 1989). Photosynthesis of each individual leaf is calculated independently using the Farquhar model for C3 plants and explicitly considering the mesophyll-bundle sheath carbon exchange for C4 plants at hourly time step (Farquhar et al., 1980; Grant, 1989a) with specific azimuth, leaf inclination, exposure of light conditions (i.e., sunlit and shaded leaves), and canopy height. The canopy stomatal resistance ($r_c$) is controlled by canopy turgor potential ($\psi_t = \psi_c$ - $\psi_{\pi p}$, where $\psi_t$, $\psi_c$, and $\psi_{\pi p}$ represent canopy turgor potential, total water potential, and osmotic potential, respectively) and canopy photosynthesis (Eq. 4) (Grant, 1995; Grant et al., 1993). $\psi_c$ is calculated through explicitly modeling the plant hydraulics, i.e., by balancing the root water uptake from different soil layers with that transferred from root to canopy, and transpired from the canopy to the atmosphere (Grant, 1995). Canopy photosynthesis is calculated by summing the photosynthesis of all individual leaves, and is coupled with the calculation of canopy stomatal resistance as:

$$r_{cmin} = 0.64(C_b - C_i^{'})/V_c^{'} \quad r_c \text{ driven by rates of carboxylation } vs. \text{ diffusion} \tag{4a}$$

$$r_c = r_{cmin} + (r_{cmax} - r_{cmin})e^{(-\beta\psi_t)} \quad r_c \text{ constrained by water status} \tag{4b}$$

where $r_c$ is canopy stomatal resistance to vapor flux, $r_{cmin}$ is the minimum $r_c$ at $\psi_c = 0$ MPa, $C_b$ is the $CO_2$ concentration in canopy air, $C_i$' is the intercellular $CO_2$ concentration at $\psi_c = 0$ MPa, $V_c$' is the potential canopy $CO_2$ fixation rate at $\psi_c = 0$ MPa, $r_{cmax}$ is canopy cuticular resistance to vapor flux, and $\beta$ is the stomatal resistance shape parameter.

### 2.1.2. Carbon allocation, crop yield, and autotrophic respiration (Ra)

*Ecosys* simulates phenologically-driven plant carbon allocation to shoot and root (Grant, 1989b, 1989c). The dynamic ratio of shoot and root carbon allocation are functions of the number of phyllochron intervals and of the water and nutrient status of the plant (Grant, 1989b). The allocated carbohydrate will be first used for maintenance respiration (*Rm*) in both shoot and root, which is calculated based on the canopy temperature (shoot)/soil temperature (root), shoot/root dry biomass, and nutrient stoichiometry. If the allocated carbohydrate can not meet the maintenance respiration, the unmet requirement is remobilized from the existing foliage carbohydrate pool, driving leaf senescence. Remaining carbohydrate after subtracting the maintenance respiration from total carbohydrate is used for growth respiration (*Rg*) and dry mass (DM) formation. For shoots, DM is partitioned to as many as seven organs, including leaf, sheath, stalk, soluble reserves, husk, cob, and grain, with dynamic partitioning coefficients varying with growth stages (Grant, 1989b). Before floral induction, the shoot DM only consists of leaf and sheath compartments. After floral induction and before anthesis, the shoot DM is allocated to all seven compartments except grain, which begins after anthesis, with partition coefficients calculated from organ growth curves (Grant, 1989b). The modelled yield upon harvest is determined by the seed number and kernel mass set during pre- and post-anthesis growth stages. The plant growth status during stem elongation and the length of post anthesis period together determine the seed number formulation. The kernel mass is determined by the seed growth during the early grain filling stage, limited by the predefined maximum kernel mass (Grant et al., 2011). The grain filling rate in *ecosys* is limited by canopy temperature, and soluble reserve carbon and reserve nutrients in the grain.

### 2.1.3. Heterotrophic respiration (Rh) and soil carbon dynamics

*Ecosys* computes Rh with explicit microbial dynamics that considers the stoichiometric interactions among carbon, nitrogen and phosphorus (Grant, 2013; Grant and Rochette, 1994). Specifically, organic matter and their transformation occur in five organic matter-microbial complexes, which are coarse woody litter, fine nonwoody litter (including root exudates), animal manure (if applied), particulate organic matter (POM) and humus. Each complex has five organic states, including solid organic matter, sorbed organic matter, microbial residue, dissolved organic matter, and the decomposition agents (microbes), all of which are vertically resolved from the surface litter layer to the bottom of the soil column. The microbes include diverse functional groups, such as obligate aerobes (bacteria and fungi), aerobic and facultative nitrifiers, facultative anaerobes (denitrifiers), obligate anaerobes (fermenters), heterotrophic (acetotrophic) and autotrophic (hydrogenotrophic) methanogens, and aerobic and anaerobic heterotrophic diazotrophs (non-symbiotic $N_2$ fixers). In computing the organic matter transformation, solid organic matter is first decomposed by microbes as a function of active microbial biomass (as an approximation to the exoenzyme hydrolysis), the product (aka soluble organic matter) is then taken up by microbes in the presence of mineral soil sorption to support microbial catabolic activity (i.e., heterotrophic respiration), which drives microbial biomass growth and mortality. Mineralization associated with heterotrophic respiration produces ammonium, $CO_2$ and inorganic phosphorus to drive the metabolism of lithotrophic groups. To maintain the elemental stoichiometry, all microbial groups compete with plants for inorganic nutrients, such as ammonium, nitrate and dissolved inorganic phosphorus. Besides, aerobic microbes also compete with plant roots for oxygen. Therefore, the heterotrophic respiration simulated by *ecosys* comprehensively resolves important process constraints from microbial population dynamics, organic matter formation and destabilization, nutrient limitation and plant-microbial interaction as influenced by the soil physical conditions. Mechanistically, *ecosys* is well positioned to conduct a comprehensive assessment of SOC change and greenhouse gas budget of agroecosystems. More details on the soil biogeochemistry in *ecosys* can be found at Grant (2014).

## 2.2. Model setup

### 2.2.1. Site-scale simulation, calibration, and validation

We evaluated the performance of *ecosys* using seven agricultural sites from the AmeriFlux network (https://ameriflux.lbl.gov/) that span a wide range of climate and soil conditions (Fig. 1b and Table 1) located in the U.S. Midwest. Among these sites, US-Ne1 planted corn during the study period, whereas other sites had corn-soybean rotations; US-Ne1 and US-Ne2 are irrigated sites, whereas other sites are rainfed. Ecosystem $CO_2$, water, and energy fluxes were measured using the eddy covariance technique at these sites (Baldocchi et al., 2001; Baldocchi, 2003).

The hourly gap-filled meteorological variables (i.e., air temperature, precipitation, downward shortwave radiation, humidity, and wind speed) from AmeriFlux and soil information (i.e., bulk density (BD), field capacity (FC), wilting point (WP), soil texture, saturated hydraulic conductivity (KSat), soil organic carbon (SOC), pH, and cation exchange capacity (CEC)) from the Gridded Soil Survey Geographic Database (gSSURGO) at these sites were used to drive *ecosys*. For US-Ne1, US-Ne2 and US-Ne3, detailed land management practices (including planting time and density, irrigation and fertilizer time and amount, tillage time and intensity) from the site records were also available as inputs for the model. For other sites, we used 7.5 plants/$m^2$ and 37.1 plants/$m^2$ for corn and soybean with the planting date from the Risk Management Agency (RMA) of United States Department of Agriculture (USDA) (Lobell et al., 2014), and applied 18 gN/$m^2$/year fertilizer before planting for corn years.

The time series of GPP, NEE, and Reco of US-Ne sites during 2001–2012 were obtained from the FLUXNET2015 Tier 1 dataset (http://fluxnet.fluxdata.org/data/fluxnet2015-dataset/), and the LAI and carbon allocation data at different growth stages for those three sites during 2003–2012 were obtained from Carbon Sequestration Program (CSP) at University of Nebraska-Lincoln's Agricultural Research and Development Center (http://csp.unl.edu/Public/sites.htm). For other

**Table 1**
Site information of selected eddy-covariance sites in the U.S. Midwest for model evaluation.

| Site | Latitude | Longitude | MAT(°C) | MAP(mm) | Simulated Period | Site Condition | Crop Types | References |
|---|---|---|---|---|---|---|---|---|
| **US-Ne1** | 41.17 | -96.48 | 10.4 | 710 | 2001-2012 | Irrigated | Continuous corn | (Suyker et al., 2005; Suyker and Verma, 2012; Verma et al., 2005) |
| **US-Ne2** | 41.16 | -96.47 | 10.4 | 710 | 2001-2012 | Irrigated | Soybean in even years before 2009, corn in other years | (Suyker et al., 2005; Suyker and Verma, 2012; Verma et al., 2005) |
| **US-Ne3** | 41.17 | -96.44 | 10.4 | 710 | 2001-2012 | Rainfed | Corn in odd years and soybean in even years | (Suyker et al., 2005; Suyker and Verma, 2012; Verma et al., 2005) |
| **US-Bo1** | 40.01 | -88.29 | 11.5 | 821 | 2001-2008 | Rainfed | Corn in odd years and soybean in even years | (Bernacchi et al., 2005; Meyers, 2004) |
| **US-Br1** | 41.69 | -93.69 | 9.1 | 938 | 2005-2011 | Rainfed | Corn in odd years and soybean in even years | (Hernandez-Ramirez et al., 2011) |
| **US-Ib1** | 41.86 | -88.22 | 9.5 | 972 | 2005-2011 | Rainfed | Corn in even years and soybean in odd years | (Allison et al., 2005) |
| **US-Ro1** | 44.71 | -93.09 | 7.7 | 764 | 2004-2012 | Rainfed | Corn in odd years and soybean in even years | (Baker and Griffis, 2005; Griffis et al., 2008) |

four sites, the gap-filled GPP, NEE, Reco, and LAI from the AmeriFlux website were used for the model evaluation. We fine tuned the rubisco carboxylation activity and plant maturity group parameters of corn and soybean to match the seasonal patterns and magnitude of GPP and LAI at US-Ne1, US-Ne2 and US-Ne3 sites. The tuned model was evaluated at US-Ne sites using NEE, Reco, and carbon allocation measurements, and at other sites using the observed GPP, NEE, Reco, and LAI data.

### *2.2.2. Regional-scale crop yield and GPP simulation, calibration, and validation*

For regional-scale simulations, we focused on the three I states (Illinois, Indiana, and Iowa), which is the major corn and soybean production area of the U.S. We conducted simulations at each county within three I states from 2001 to 2018 using corn-soybean rotation without irrigation (the major planting strategies within this area), with the North American Land Data Assimilation System (NLDAS-2) hourly meteorological data and gSSURGO soil data as inputs. NLDAS-2 meteorological data is from the integration of observation-based and model reanalysis data, with 0.125° spatial resolution covering central North America. The county scale meteorological variables were aggregated from the NLDAS-2 grids within that county. The National 2020 Cultivated Layer (based on 2016-2020 USDA Cropland Data Layer) (USDA, 2021) and gSSURGO datasets were used to obtain the county-scale soil properties (i.e., BD, soil texture, WP, FC, KSat, SOC, pH, and CEC) that correspond to the county-scale cropland majority soil type. For regional scale simulations, corn and soybean were also planted with 7.5 plants/$m^2$ and 37.1 plants/$m^2$ at the county scale based on the RMA planting date (2001–2012) (Lobell et al., 2014) and the state-scale/agricultural district-scale crop progress reports (2013–2018) depending on the data availability (Figure S4), and all crops were harvested on October 31. The state-wise crop specific fertilizer information provided by USDA (USDA, 2019) was applied in the simulations.

For model calibration and evaluation, we used county-scale rainfed corn and soybean yield from USDA National Agricultural Statistics Service (NASS), and a new 250m resolution daily GPP estimation using MODIS-based soil-adjusted near-infrared reflectance of vegetation (SANIRv) and photosynthetically active radiation (PAR) (Jiang et al., 2021). The fixed linear yield trend was calculated from the NASS crop yield data for corn and soybean respectively for each county, and was used to adjust the simulated yield to year 2009 (the midpoint of 2001-2018). To constrain *ecosys* efficiently, we built surrogate models for crop yield and GPP separately using the Long Short Term Memory networks (LSTM) to predict daily GPP and end-of-seasonal crop yield under different corn and soybean parameters. In these models, the daily climate meteorological data, three layers soil parameters (i.e., 0-5, 5-30, and 30-100 cm), crop type, corn parameters, soybean parameters, fertilizer amount, planting and harvest date, and day of year (DOY) were used as inputs, and GPP or crop yield were used as output, respectively. The RMSE of the surrogate models were 13.5 gC/$m^2$ and 0.46 gC/$m^2$/day for yield and GPP, respectively. The parameters for soybean include rubisco carboxylation activity, plant maturity group, maximum number of fruiting sites per reproductive node, and maximum rate of kernel filling; and for corn include fraction of leaf protein in bundle sheath chlorophyll, plant maturity group, maximum number of fruiting sites per reproductive node, and maximum rate of kernel filling. We conducted the parameter calibration for each county based on the surrogate models, and used data from even years during 2001 to 2018 for model constraint and those from odd years for model validation. In applying the constraint, the difference between simulated and observed yield, accumulated growing season (i.e., May to September) GPP, and monthly growing season GPP were minimized using the cost function in Eq. (5c).

$$L(soybean) = NRMSE_{yield}(soybean) + NRMSE_{GPP}(soybean) + NRMSE_{GPP\_monthly}(soybean) \quad (5a)$$

$$L(corn) = NRMSE_{yield}(corn) + NRMSE_{GPP}(corn) + NRMSE_{GPP\_monthly}(corn) \tag{5b}$$

$$L = L(soybean) + L(corn) \tag{5c}$$

where $NRMSE_{yield}$(soybean) and $NRMSE_{yield}(corn)$ are normalized RMSE of model simulated and measured crop yield for corn and soybean, respectively based on Eq. (6); $NRMSE_{GPP}$(soybean) and $NRMSE_{GPP}(corn)$ are normalized RMSE of model simulated and measured growing season accumulated GPP for corn and soybean, respectively based on Eq. (7); $NRMSE_{GPP\_monthly}$(soybean) and $NRMSE_{GPP\_monthly}(corn)$ are normalized RMSE of model simulated and measured multi-year averaged growing season monthly GPP for corn and soybean, respectively based on Eq. (8).

$$NRMSE_{yield} = \frac{\sqrt{\frac{1}{9}\sum_{year=even\_years}\left(Yield_{sim(year)} - Yield_{obs(year)}\right)^2}}{\frac{1}{9}\sum_{year=even\_years}Yield_{obs(year)}} \tag{6}$$

$$NRMSE_{GPP} = \frac{\sqrt{\frac{1}{9}\sum\limits_{year=even\_years}\left(GPP_{sim(year)} - GPP_{obs(year)}\right)^2}}{\frac{1}{9}\sum\limits_{year=even\_years}GPP_{obs(year)}} \tag{7}$$

$$NRMSE_{GPP\_monthly} = \frac{\sqrt{\frac{1}{5}\sum\limits_{month=5}^{9}\left(\frac{\left(\sum\limits_{year=even\_years}\left(GPP_{sim(year,month)} - GPP_{obs(year,month)}\right)\right)}{9}\right)^2}}{\frac{1}{45}\sum\limits_{year=even\_years}\sum\limits_{month=5}^{9}GPP_{obs(year,month)}} \tag{8}$$

where $Yield_{sim(year)}$ and $Yield_{obs(year)}$ are the simulated and observed yield, $GPP_{sim(year)}$ and $GPP_{obs(year)}$ are the simulated and observed growing season accumulated GPP, $GPP_{sim(year,month)}$ and $GPP_{obs(year,month)}$ are the simulated and observed GPP at certain month, *even_years* is the years used for model constrain (i.e., 2002, 2004, ..., 2018).

## 3. Results

### 3.1. Site-scale validation of ecosys in simulating carbon dynamics

We compared observed and modelled GPP, NEE, Reco fluxes at 7 eddy-covariance sites in the U.S. Midwest (Fig. 1b). The results indicate that *ecosys* can capture both the magnitude and seasonal patterns of

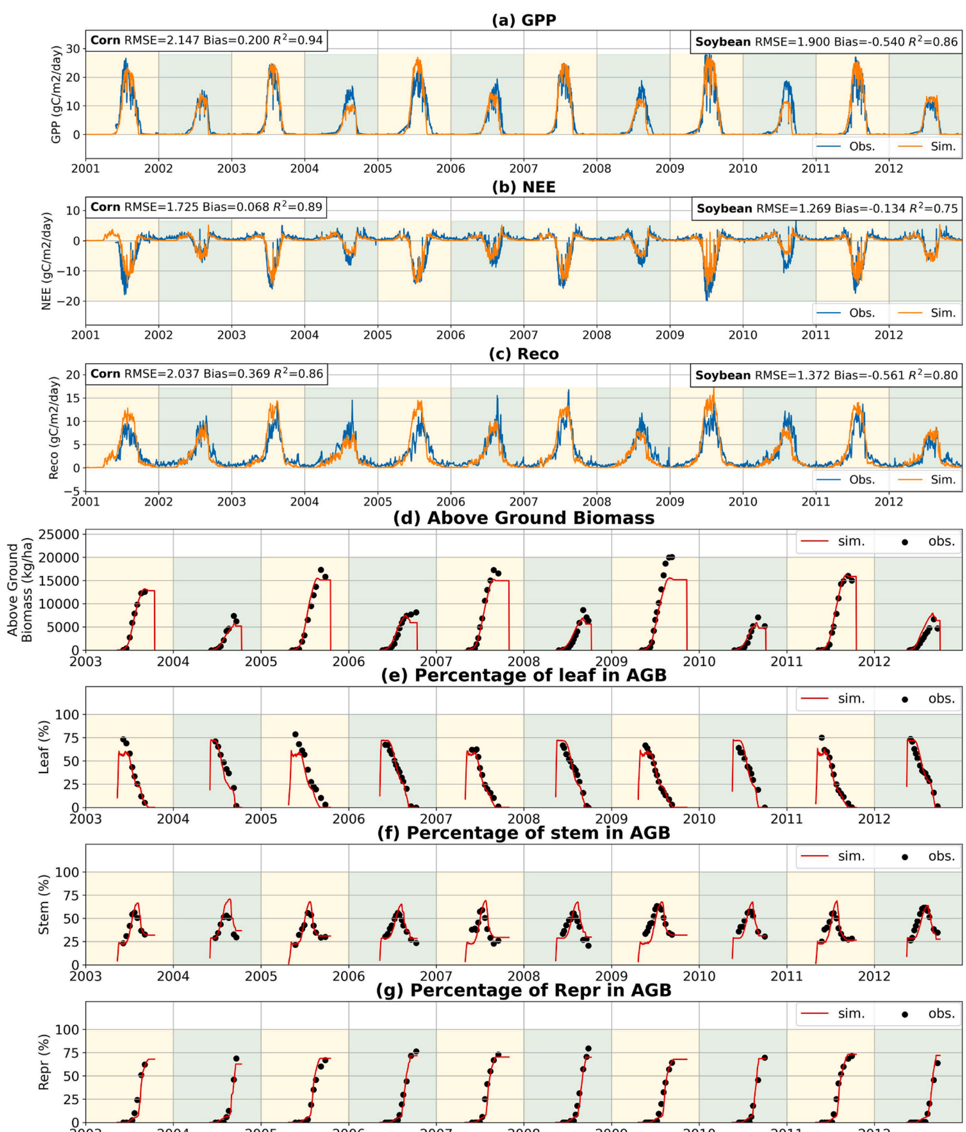


**Fig. 2.** Comparing *ecosys* simulated GPP, NEE, Reco and carbon allocation with site observations at US-Ne3 site in Nebraska for both corn (light yellow shaded) and soybean (light blue shaded).

these carbon fluxes with high accuracy at both daily and monthly scales (i.e., Figs. 2, 3, S1, S2, and Table 2). The simulated GPP is consistent with the observations for both corn and soybean throughout the growing season, and can reflect the magnitude difference between corn and soybean during peak growing season. At the daily scale, $R^2$ and RMSE are 0.94 and 2.15 gC/m$^2$/day for corn, and are 0.86 and 1.90 gC/m$^2$/day for soybean at US-Ne3, respectively (Fig. 2a). The seasonal pattern and magnitude of Reco, which is high during summer and low during winter in the U.S. Midwest, can be captured by *ecosys* for both corn and soybean with high modeling skills (i.e., $R^2$=0.86 and RMSE=2.04 gC/m$^2$/day for corn, and $R^2$=0.80 and RMSE=1.37 gC/m$^2$/day for soybean at US-Ne3, Fig. 2c). As for NEE, the magnitude, peaking time, and zero-crossing points in observations are all captured by *ecosys* with $R^2$=0.89 and RMSE=1.73 gC/m$^2$/day for corn, and $R^2$=0.75 and RMSE=1.27 gC/m$^2$/day for soybean, respectively, at US-Ne3 (Fig. 2b).

The comparison of observed and modelled above ground biomass (AGB) and its partition showed that the dynamics of AGB and its allocation to leaf, stem, and reproductive organs can be reproduced by *ecosys* for both corn and soybean, ensuring the application of *ecosys* for crop yield simulation (Figs. 2, S1, and S2). The $R^2$ between the measured and simulated AGB and its leaf, stem, and reproductive percentages are 0.95, 0.92, 0.60, and 0.94 at US-Ne3. In both observations and simulations, during the early growing season, the AGB increase appears mostly as leaves to increase photosynthesis; during the peak growing season, the AGB increase is mostly found in stem for plant structural support; and at the late stage, the AGB increase is mostly allocated to the reproductive organ for grain formulation.

We also compared the responses of the modelled and observed GPP, Reco, and NEE to air temperature (Ta) and vapor pressure deficit (VPD) at those eddy-covariance sites (Fig. 4 and S3). The results indicate that *ecosys* captured the responses of major carbon fluxes, e.g., GPP, Reco and NEE to variations in air temperature and VPD at the eddy-covariance sites reasonably well. Taking corn as an example, when Ta is less than 30°C, GPP increases quickly, but stays stable when Ta becomes higher. Both observations and simulations show such a response, which is primarily controlled by the limitation of temperature on leaf rubisco activity. As for the response of GPP to VPD, GPP increases when VPD is small, but decreases when VPD gets higher in both observations and simulations, which reveals the emergent influence of VPD on crop stomatal conductance. The observed Reco showed a strong response to Ta (i.e., increases quickly with higher Ta when Ta is below the optimal value) and no significant response to VPD, which can also be captured by *ecosys* simulations. As for NEE, the balance of carbon fixation and respiration, shows similar responses to Ta and VPD as that of GPP in both observations and simulations. The reason that results in the similar response of NEE and GPP to environmental factors is that NEE is dominated by crop photosynthesis during peak growing season. Similar responses of GPP, NEE, and Reco to Ta and VPD are also captured by *ecosys* simulations for soybean at the eddy-covariance sites (Fig. S3).

### 3.2. Regional-scale crop yield and gross primary productivity simulation

#### 3.2.1. Regional-scale corn and soybean yield simulation

The comparison between modelled and NASS reported crop yield shows that *ecosys* can reproduce the spatial distribution and interannual variability of crop yield over three I States for both corn and soybean

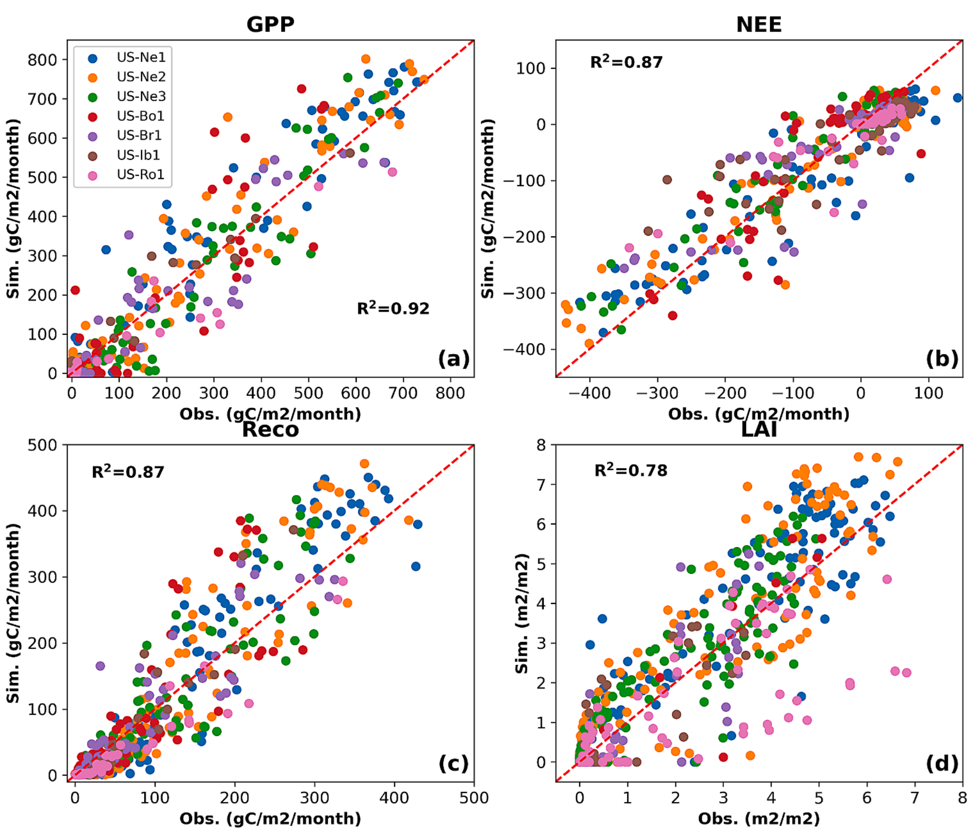


**Fig. 3.** Comparison of simulated and observed carbon fluxes (monthly) and LAI at the eddy-covariance sites. Red dashed lines indicate the 1-to-1 line.

**Table 2**
Comparison statistics of *ecosys* simulated daily surface carbon fluxes with eddy-covariance sites observations.

| Sites | NEE | | | GPP | | | Reco | | |
|---|---|---|---|---|---|---|---|---|---|
| | RMSE(gC/m²/day) | Bias(gC/m²/day) | $R^2$ | RMSE(gC/m²/day) | Bias(gC/m²/day) | $R^2$ | RMSE(gC/m²/day) | Bias(gC/m²/day) | $R^2$ |
| **US-Ne1** | 1.96 | -0.60 | 0.86 | 2.44 | 0.67 | 0.93 | 1.92 | -0.07 | 0.87 |
| **US-Ne2** | 1.67 | -0.28 | 0.88 | 2.32 | 0.25 | 0.92 | 1.98 | -0.03 | 0.83 |
| **US-Ne3** | 1.51 | -0.04 | 0.86 | 2.02 | -0.18 | 0.91 | 1.72 | -0.11 | 0.79 |
| **US-Bo1** | 2.26 | 0.11 | 0.65 | 3.31 | 0.06 | 0.74 | 2.04 | 0.21 | 0.67 |
| **US-Br1** | 2.34 | 0.04 | 0.59 | 2.66 | -0.06 | 0.80 | 1.46 | -0.01 | 0.77 |
| **US-Ib1** | 1.90 | -0.35 | 0.69 | 1.64 | 0.28 | 0.91 | 1.66 | 0.05 | 0.77 |
| **US-Ro1** | 1.77 | -0.15 | 0.69 | 2.12 | -0.69 | 0.89 | 1.30 | -0.78 | 0.89 |

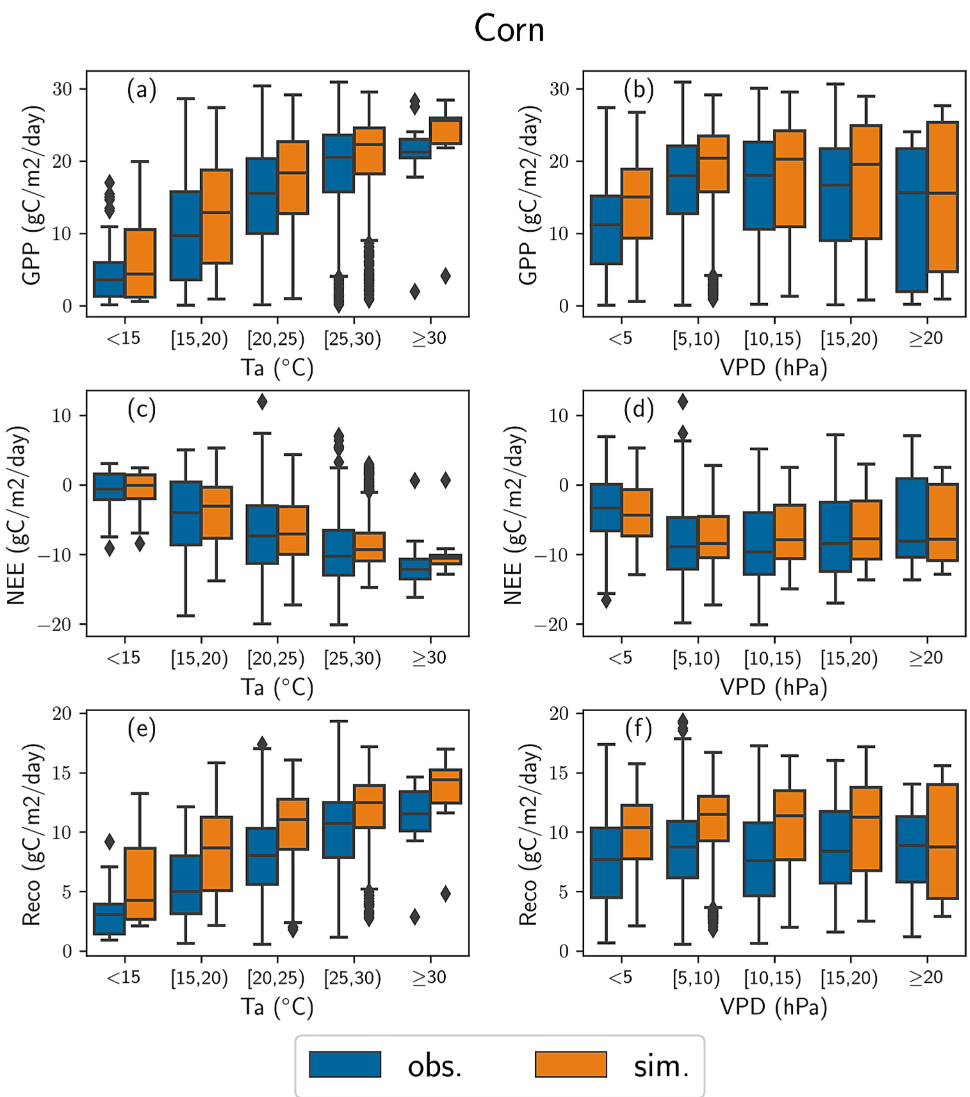


**Fig. 4.** Responses of simulated and observed daily GPP, NEE, and Reco to air temperature and VPD for corn during peak growing season (June to August).

(Figs. 5, S5-7). Modeled long-term (2001–2018) averaged crop yield and NASS ground truth shows similar spatial patterns over three I States during both calibration years and validation years for both corn and soybean. The $R^2$, RMSE, and bias between the spatial patterns of modelled and measured yield are 0.83, 8.23 Bu/Acre, and 2.72 Bu/Acre for corn, and 0.80, 2.39 Bu/Acre, and 0.07 Bu/Acre for soybean, respectively. Long-term averaged corn and soybean yield in the northern part of three I States are higher than that of the southern part in both observations and simulations, which may be caused by the differences in soil (i.e., higher SOC in the northern part) and climate conditions (i.e., more frequent heat stress and extreme precipitation events in the southern part). The temporal variation of simulated average yield during 2001 to 2018 is also consistent with the observations with $R^2$ of 0.83 and 0.63 for corn and soybean, respectively.

### 3.2.2. Regional-scale corn and soybean GPP simulation

We also compared the modeled long-term averaged GPP and a new satellite-based GPP estimation during the peak growing season (June to August). The spatial patterns of simulated and NIRv-based peak growing season accumulated GPP are similar during calibration years and validation years for both corn and soybean (Fig. 6), which are consistent with the spatial patterns of yield (Fig. 5). The $R^2$, relative RMSE between

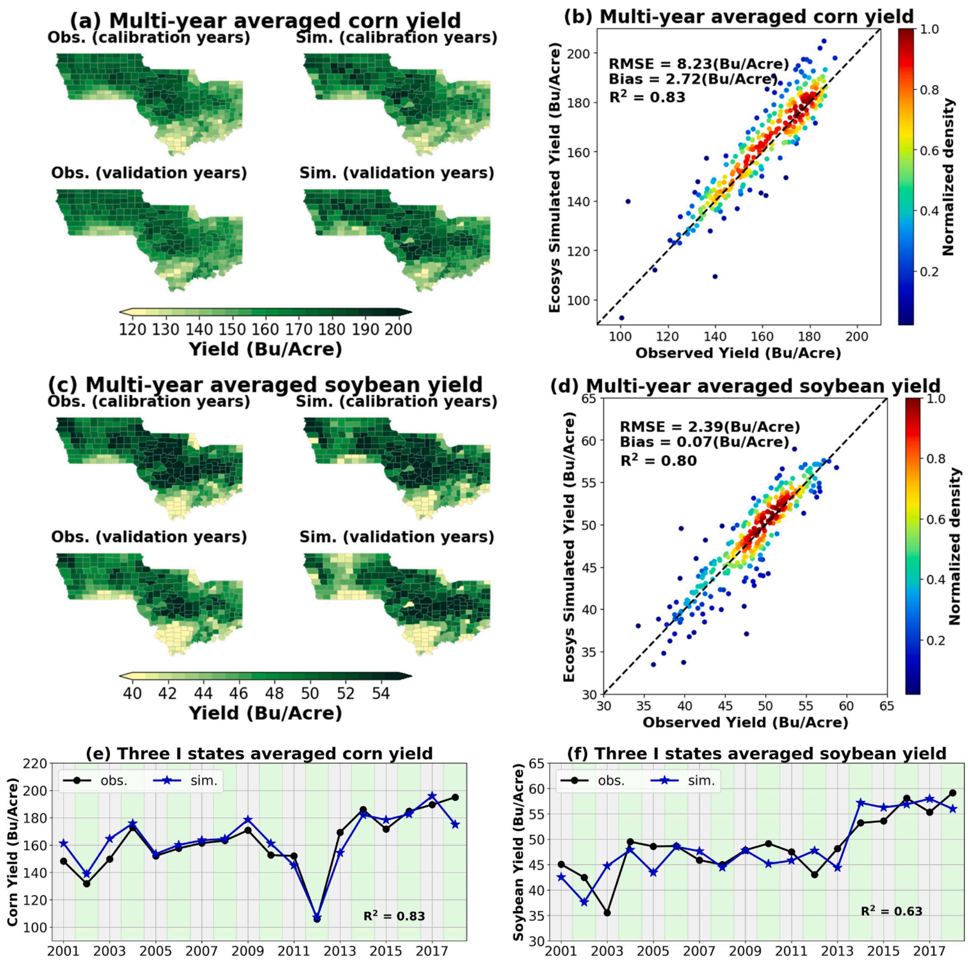


**Fig. 5.** Comparison of *ecosys* simulated crop yield and NASS reported crop yield. (a) Spatial patterns of simulated and observed multi-year averaged corn yield in calibration and validation years. (b) Density scatter plot of simulated and observed multi-year averaged corn yield. Different colors mean the ratio of points density to maximum points density, similar for the density scatter plots in other figures. (c) Spatial patterns of simulated and observed multi-year averaged soybean yield in calibration and validation years. (d) Density scatter plot of simulated and observed multi-year averaged soybean yield. (e) and (f) is the time series of three I states averaged corn and soybean yield respectively. Light green shaded years in (e) and (f) are calibration years, and grey shaded years are validation years.

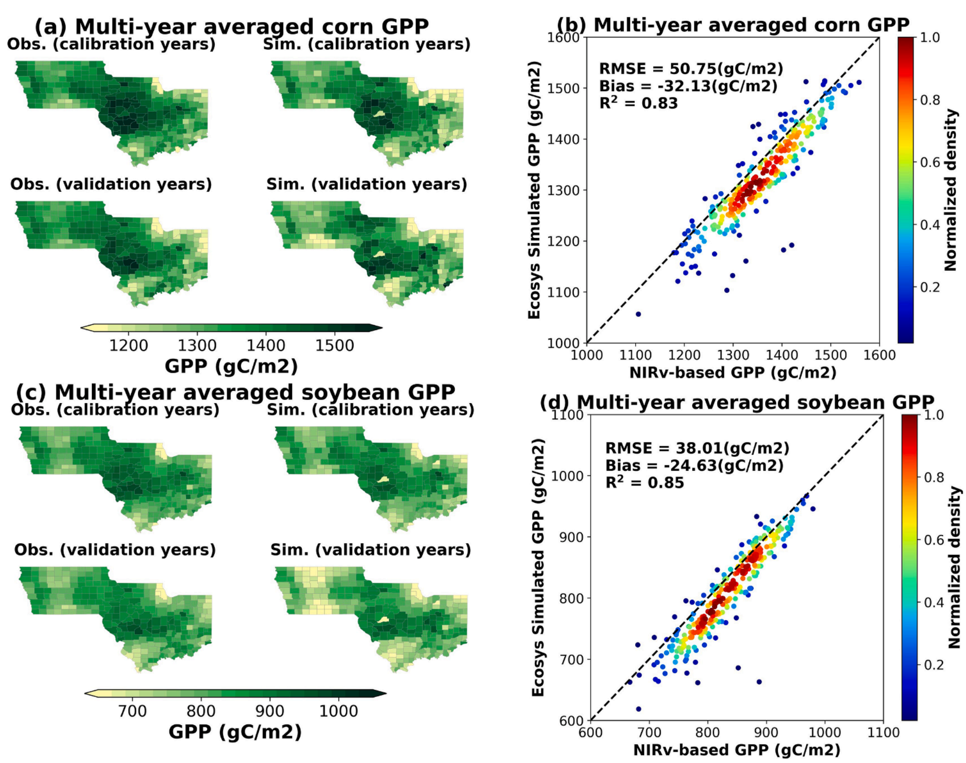


**Fig. 6.** Comparison of *ecosys* simulated peak growing season accumulated (June to August) GPP and NIRv-based GPP. (a) Spatial patterns of simulated and NIRv-based multi-year averaged corn GPP in calibration and validation years. (b) Density scatter plot of simulated and NIRv-based multi-year averaged corn GPP. (c) Spatial patterns of simulated and NIRv-based multi-year averaged soybean GPP in calibration and validation years. (d) Density scatter plot of simulated and NIRv-based multi-year average soybean GPP.

the spatial patterns of modelled and NIRv-based GPP are 0.83 and 3.7% for corn, and 0.85 and 4.6% for soybean, respectively. The seasonal variation of GPP for both corn and soybean can also be captured by *ecosys* at regional scale when benchmarked with NIRv-based GPP (Fig. 7, S8, and S10). For example, GPP of corn and soybean grows quickly from June to July, and peaks at July and August in both simulations and NIRv-based observations (Fig. 7).

### 3.3. Response of crop yield to environmental variability in the U.S. Midwest

Besides comparing the absolute value of modelled and observed yield and GPP, we also investigated the response of these variables to the environmental factors to evaluate whether the model can capture such response (Figs. 8, 9, and S12). The LOWESS (LOcally Weighted Scatterplot Smoothing) was used to fit the response of observed and modelled crop yield to key environmental factors, including Ta, precipitation, VPD, soil water content (SWC), bulk density, and SOC, in the U.S. Midwest for corn and soybean during the growing season (Fig. 8).

We found that the trend and inflection points of the observation-based response curves can be simulated by *ecosys* at the regional scale for most of the months for climate variables and different depths for soil properties, demonstrating the ability of *ecosys* in capturing the response of crop yield to environmental variabilities in the U.S. Midwest. Both observations and simulations show that yield increases with increasing Ta until an optimal Ta value, and then decreases with higher Ta. The yield~Ta response is caused by the plant enzyme and growth activity with temperature, which is also reflected in the GPP~Ta response (Fig. S12) during key growing months (i.e., July and August). For precipitation, the yield increases with increasing precipitation when

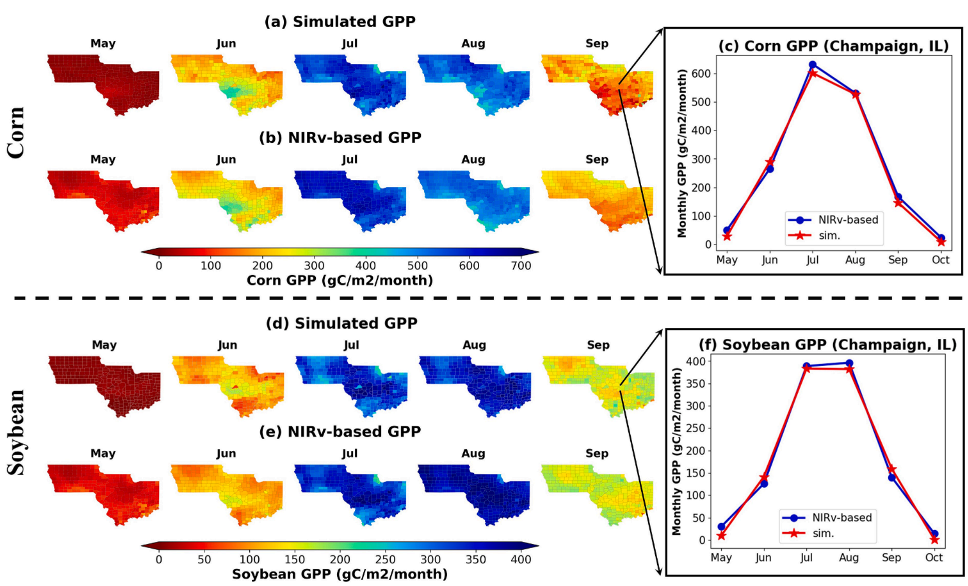


**Fig. 7.** Comparison of multi-year averaged *ecosys* simulated and NIRv-based monthly GPP for corn and soybean in validation years. (a) Simulated multi-year averaged monthly corn GPP during validation years. (b) NIRv-based multi-year averaged monthly corn GPP during validation years. (c) Comparison of simulated and NIRv-based multi-year averaged monthly corn GPP at Champaign, IL during validation years. (d) Simulated multi-year averaged monthly soybean GPP during validation years. (e) NIRv-based multi-year averaged monthly soybean GPP during validation years. (f) Comparison of simulated and NIRv-based multi-year averaged monthly soybean GPP at Champaign, IL during validation years.

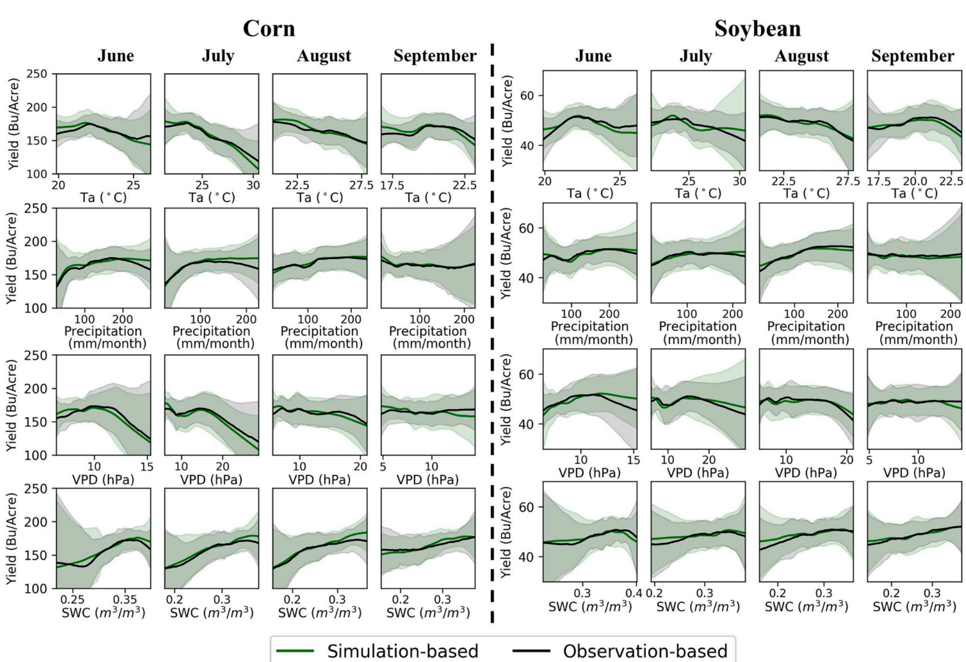


**Fig. 8.** Fitted responses of *ecosys* simulated and observed crop yield to climate variables at three I States for corn and soybean using LOWESS. The shaded regions are the 95% confidence intervals of LOWESS.

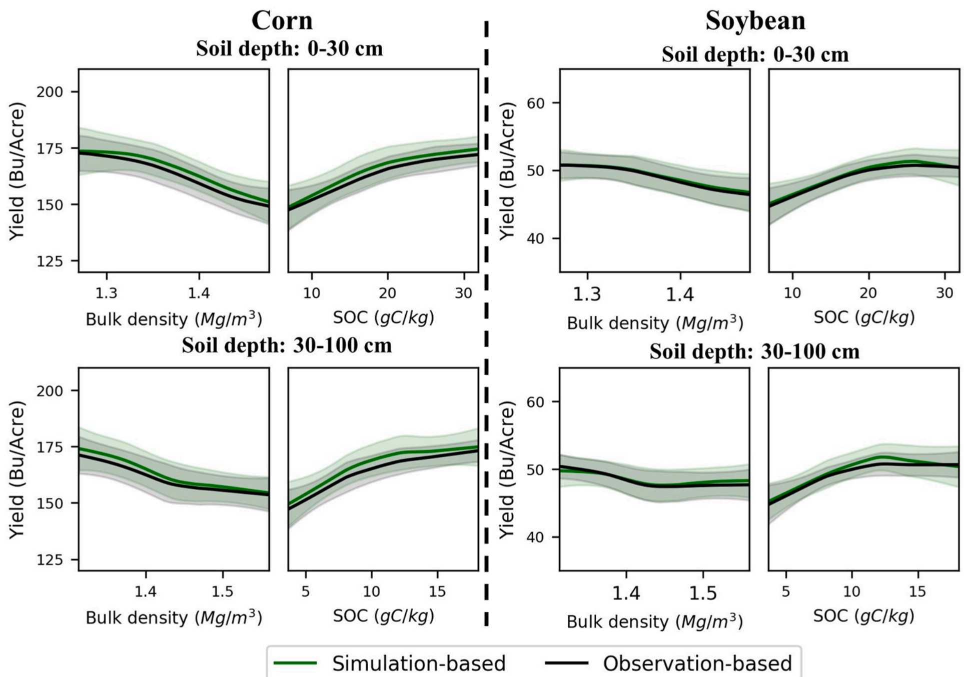


**Fig. 9.** Fitted responses of *ecosys* simulated and observed crop yield to soil conditions within different soil depths at three I States for corn and soybean using LOWESS. The shaded regions are the 95% confidence intervals of LOWESS.

precipitation is smaller and then decreases at higher precipitation, revealing the tradeoff between water limitation and excessive precipitation on crop growth (Li et al., 2019). For VPD, the yield increases with VPD when VPD is low, and decreases when VPD is higher, confirming the impacts of VPD on crop productivity in both photosynthesis (through the VPD control on stomatal conductance) (Ball, 1988; Grant et al., 1993; Zhang et al., 2021) and crop yield (Kimm et al., 2020; Lobell et al., 2014; Zhou et al., 2020). The response of yield~SWC is similar to other environmental variables, revealing the tradeoff between water supply and oxygen stress at high soil moisture on crop growth. For both observations and simulations, the multi-year averaged crop yield decreases with larger bulk density and increases with larger SOC in the U.S. Midwest.

## 4. Discussion

In this study, we used an advanced agroecosystem model, *ecosys*, to thoroughly simulate carbon budget for the U.S. Midwestern agroecosystems at both the site and regional scales. To address the gap that most previous model-based cropland carbon balance quantification studies with insufficient validations that only cover a small part of the carbon cycle components, we evaluated the model performance across a more comprehensive range of carbon cycle components, including carbon fixation, carbon allocation, and ecosystem respiration at site scale. In particular, we tested *ecosys* performance at seven majority cropland eddy-covariance sites (with 55 site-years observations) across the U.S. Midwest regarding GPP, NEE, Reco, LAI, and carbon allocation simulations. The model validation results reveal that *ecosys* can simulate the seasonal cycle and magnitude of agroecosystem carbon dynamics at different individual sites with high accuracy. Across all the sites, the $R^2$ of the simulated and observed value for GPP, NEE, Reco, and LAI were 0.92, 0.87, 0.87, and 0.78, respectively (Fig. 3). In addition, the dynamics of above ground biomass and its allocation to leaf, stem, and reproductive can be reproduced by *ecosys* (Figs. 3, S1, and S2). The overall model performance at US-Ne1, Ne2, and Ne3 sites are better than that at the other 4 sites in simulating GPP, NEE and Reco (Table 2), which may largely be attributed to the more accurate records of land management practice (i.e., planting date and planting density, tillage information, and irrigation information) at the US-Ne sites.

Since the crop cultivar (e.g., maturity group) and management practices (e.g., fertilizer application rate, planting date) may varies in spatial, and is hard to obtain the information at high resolution, we calibrated the *ecosys* model using the existing observations from both USDA survey for yield and satellite-based novel GPP estimations in even years to take the spatial variation of cultivars and management practices into account, and validated the model in odd years at the regional scale by simulating over 293 counties in the three I States. The model validation results show that *ecosys* can capture the spatial and temporal variability of crop yield as well as the magnitude and seasonal patterns of GPP for both corn and soybean across the broader regions in the U.S. Midwest. The $R^2$ of the multi-year averaged simulated and observed yield for corn and soybean is 0.83 and 0.80, respectively, showing the advanced ability of *ecosys* in capturing the crop yield spatial variance. Based on our best knowledge, such a high performance in simulating crop yield with a direct benchmark with county-level NASS data has not been achieved before (Zhang et al., 2015, 2020), which is a strong demonstration of the ability of *ecosys* in simulating the carbon cycle for agroecosystems. The interannual variability of the observed crop yield can also be matched by *ecosys* simulations, but with some deviations at some years (i.e., 2003) between the observations and simulations for soybean, which may be caused by abiotic stress, such as pest, diseases, or uncaptured environmental impacts (e.g., hail, wind storm).

To fill the gap that previous studies only focused on matching the magnitude of the simulated target variables with observations, we also corroborated the simulated and observed responses of carbon-related variables to climate and soil variabilities in both the site scale and regional scale simulations. The response of the carbon fluxes and crop yield to the environmental variabilities obtained from the observations can be captured well by *ecosys*. For the site scale simulations, the responses of the modelled and observed GPP, Reco, and NEE to the ambient climate conditions (i.e., temperature and VPD) at the eddy-covariance sites are consistent; for the regional scale simulations, the responses of simulated crop yield/GPP to the environmental factors were similar to those of the observations during the growing season (i.e., Figs. 8, 9, and S12). These results indicate the ability of *ecosys* in simulating carbon fluxes and crop yield across the border soil and weather conditions.

Through the comprehensive evaluation of the simulated carbon components with the observations (including GPP, Reco, and carbon allocation at the eddy-covariance sites, and GPP and yield at the regional scales), we are able to simulate the NBP at the regional scale (Fig. 10). The simulated multi-year averaged NBP had higher negative correlation to the SOC and NEE in the same period with *r* of -0.88 and -0.52, respectively, which indicates that both SOC stock and NEE drives NBP dynamics across space. As indicated in Eq. (3), annually, the accumulated NBP is approximately equal to ΔSOC, assuming ε (carbon leakage through runoff and methane emission) is sufficiently small. Our simulation results confirmed that using the carbon mass balance approach, we can regiously predict ΔSOC (Fig. 10b). This means that our method has the potential to be applied for quantifying annual-scale soil carbon dynamics for agroecosystems. However, cautions are given that, in being able to ensure the carbon mass balance approach work or have a low uncertainty, rigorous tests of different carbon cycle components, i.e., GPP, Reco, and harvest carbon, all should be conducted - currently no existing modeling-based study has demonstrated such a capability except this current study.

Although we had validated the ability of *ecosys* in simulating the carbon cycle processes for both crop yield and GPP, there are still some limitations in the regional scale carbon balance simulation that need to be further addressed. Specifically, in current simulations, we only focus on the case that with no tillage and no cover crop. In the U.S. Midwest, tillage and cover crop are the commonly adopted conservation practices (Deines et al., 2019; Seifert et al., 2019), and may change the soil carbon sequestration rate compared with the no till and no cover crop situation (Baker et al., 2007; Poeplau and Don, 2015). For the tillage practice, it may redistribute SOC content in the soil profile, affect the crop growth by influencing soil minimization and soil water content, and also affect ecosystem respiration especially Rh (Mehra et al., 2018). For cover crops, it may influence the SOC sequestration rate by increasing GPP during the winter period and competing the water and nutrients with the main crops in the summer (Abdalla et al., 2019). Studying the impacts of cover crop and tillage is beyond the scope of the current paper, but they are under active investigation in our other studies.

## 5. Conclusion

In conclusion, we evaluated an advanced agroecosystem model, *ecosys*, to thoroughly simulate carbon budget for the agroecosystems at 7 cropland eddy-covariance sites and 293 counties in the U.S. Midwest. Both the magnitude of simulated carbon flux/yield and their response to the environmental variabilities had been compared with that from the observations. For site scale simulations, the $R^2$ of the simulated GPP,

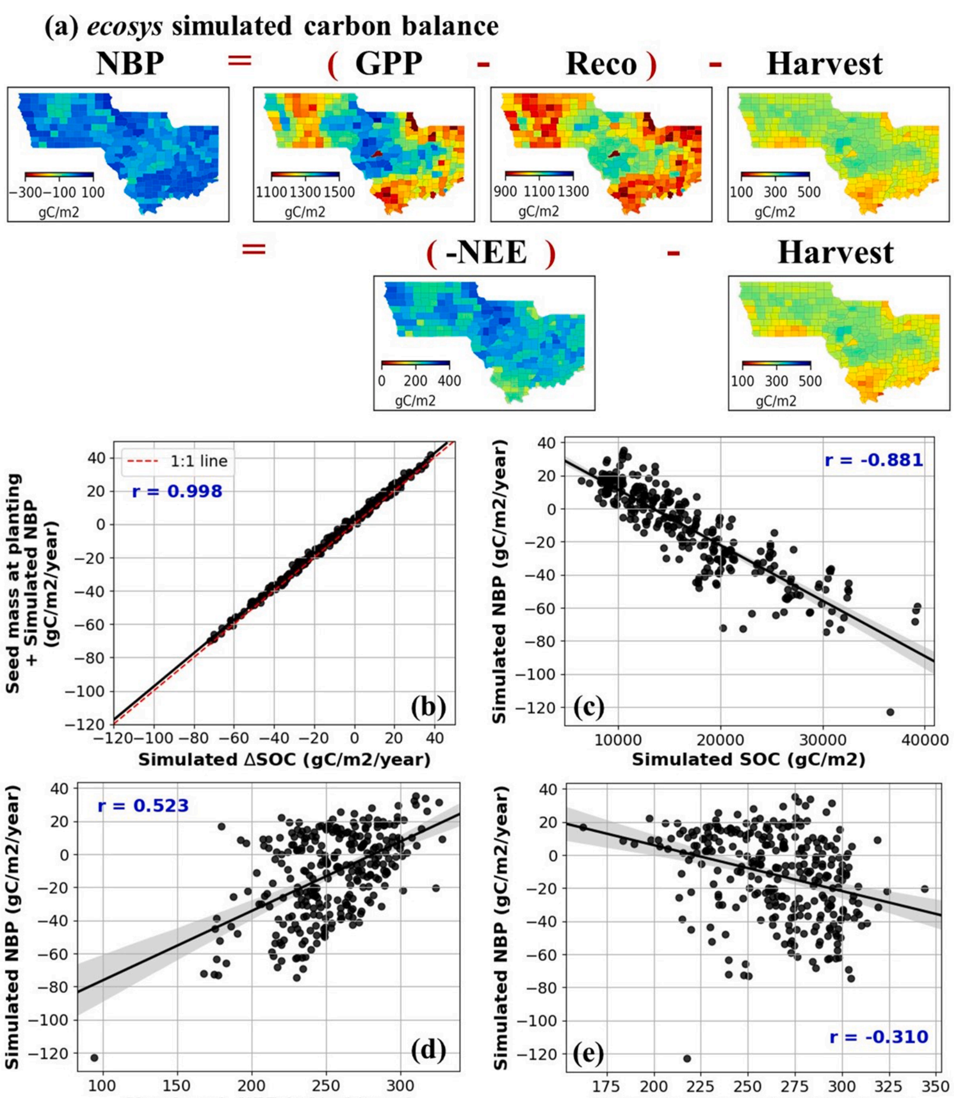


**Fig. 10.** Simulated multi-year averaged corn-soybean rotation cropland NBP during 2001-2018, and its correlation with ΔSOC, SOC content, NEE, and harvest over three I states. (a) Simulated multi-year averaged corn-soybean rotation cropland carbon budget over three I states during 2001 to 2018. (b) The scatter plot of simulated SOC change and the sum of seed mass at planting and NBP. (c) The scatter plot of averaged simulated SOC and NBP. (d) The scatter plot of simulated NEE and NBP. (e) The scatter plot of simulated harvest carbon and NBP. The black lines and shaded regions in (b)-(e) are the fitted linear regression models and the corresponding 95% confidence interval.

NEE, Reco, and LAI is 0.92, 0.87, 0.87, and 0.78, respectively. In addition, the dynamics of carbon allocation processes for both corn and soybean can also be reproduced by *ecosys*. For the regional scale simulations, the spatial pattern and interannual variance of crop yield are consistent with that from the USDA survey for both corn and soybean. Specifically, the $R^2$ of the multi-year averaged simulated and observed yield is 0.83 and 0.63 for corn and soybean, respectively; while the $R^2$ of spatial-averaged simulated and observed crop yield from 2001 to 2018 is 0.83 and 0.80 for corn and soybean, respectively. This study is a strong demonstration of the ability of *ecosys* in simulating the carbon cycle for agroecosystems. The response of carbon cycle processes/yield to the environmental variabilities obtained from the simulations is consistent with that from the observations at both site-scale and regional scale simulations, revealing the applicability of *ecosys* in simulating the impacts of future climate change on the carbon cycle of the U.S. Midwestern agroecosystems. In addition, by evaluating and constraining the majority carbon cycle process (i.e., GPP and yield at regional scale), we are able to simulate the net biome productivity, which can be applied to quantify the soil carbon dynamics of agroecosystems. The method and framework adopted in this study can also be applied to other land surface models and terrestrial biosphere models to improve the accounting of ecosystem carbon budget by integrating the mechanism models, observations, and advanced machine learning tools.

## Declaration of Competing Interest

The authors declare that they have no known competing financial interests or personal relationships that could have appeared to influence the work reported in this paper.

## Acknowledgement

Authors acknowledge the support from the National Science Foundation (NSF) Career Award (1847334), the Foundation for Food and Agriculture Research (FFAR) (Grant ID: 602757), DOE Advanced Research Projects Agency-Energy (ARPA-E) SMARTFARM program (DE-FOA-0002250), NASA Carbon Monitoring System Program (80NSSC18K0170), USDA National Institute of Food and Agriculture (NIFA) Program (2017-67013-26253 and Hatch), and Department of Energy (DOE) (25-1215-0208-006). The content of this publication is solely the responsibility of the authors and does not necessarily represent the official views of the FFAR. The views and opinions of authors expressed herein do not necessarily state or reflect those of the United States Government or any agency thereof. We thank Andrew Suyker from University of Nebraska Lincoln for providing the crop growth data at the Nebraska Mead flux-tower sites, and Junrui Ni from University of Illinois for processing the USDA crop planting date data at Illinois, Iowa, and Indiana. We acknowledge the following AmeriFlux sites for their data records: US-Ne1, US-Ne1, US-Ne3, US-Bo1, US-Br1, US-Ib1, and US-Ro1. Funding for AmeriFlux data resources was provided by the U.S. DOE's Office of Science.

## Supplementary materials

Supplementary data associated with this article can be found, in the online version, at doi:10.1016/j.agrformet.2021.108521.

## References

Abdalla, M., Hastings, A., Cheng, K., Yue, Q., Chadwick, D., Espenberg, M., Truu, J., Rees, R.M., Smith, P., 2019. A critical review of the impacts of cover crops on nitrogen leaching, net greenhouse gas balance and crop productivity. Glob. Chang. Biol. 25, 2530–2543. https://doi.org/10.1111/gcb.14644.

Allison, V.J., Michael Miller, R., Jastrow, J.D., Matamala, R., Zak, D.R., 2005. Changes in soil microbial community structure in a tallgrass prairie chronosequence. Soil Sci. Soc. Am. J. https://doi.org/10.2136/sssaj2004.0252.

Anderson, J.P.E., Domsch, K.H., 1975. Measurement of bacterial and fungal contributions to respiration of selected agricultural and forest soils. Can. J. Microbiol. 21, 314–322. https://doi.org/10.1139/m75-045.

Baker, J.M., Griffis, T.J., 2005. Examining strategies to improve the carbon balance of corn/soybean agriculture using eddy covariance and mass balance techniques. Agric. For. Meteorol. https://doi.org/10.1016/j.agrformet.2004.11.005.

Baker, J.M., Ochsner, T.E., Venterea, R.T., Griffis, T.J., 2007. Tillage and soil carbon sequestration—what do we really know? Agric. Ecosyst. Environ. 118, 1–5. https://doi.org/10.1016/j.agee.2006.05.014.

Baldocchi, D.D., 2003. Assessing the eddy covariance technique for evaluating carbon dioxide exchange rates of ecosystems: past, present and future. Global Change Biol. https://doi.org/10.1046/j.1365-2486.2003.00629.x.

Baldocchi, D., Falge, E., Gu, L., Olson, R., Hollinger, D., Running, S., Anthoni, P., Bernhofer, C., Davis, K., Evans, R., Fuentes, J., Goldstein, A., Katul, G., Law, B., Lee, X., Malhi, Y., Meyers, T., Munger, W., Oechel, W., Paw, K.T., Pilegaard, K., Schmid, H.P., Valentini, R., Verma, S., Vesala, T., Wilson, K., Wofsy, S., 2001. FLUXNET: a new tool to study the temporal and spatial variability of ecosystem–scale carbon dioxide, water vapor, and energy flux densities. Bull. Am. Meteorol. Soc. doi:2.3.co;2">10.1175/1520-0477(2001)082<2415:fantts>2.3.co;2.

Ball, J.T., 1988. An Analysis of Stomatal Conductance.

Bardgett, R.D., McAlister, E., 1999. The measurement of soil fungal:bacterial biomass ratios as an indicator of ecosystem self-regulation in temperate meadow grasslands. Biol. Fertil. Soils 29, 282–290. https://doi.org/10.1007/s003740050554.

Bernacchi, C.J., Hollinger, S.E., Meyers, T., 2005. The conversion of the corn/soybean ecosystem to no-till agriculture may result in a carbon sink. Global Change Biol. https://doi.org/10.1111/j.1365-2486.2005.01050.x.

Blanco-Canqui, H., Lal, R., 2004. Mechanisms of carbon sequestration in soil aggregates. Crit. Rev. Plant Sci. https://doi.org/10.1080/07352680490886842.

Brilli, L., Bechini, L., Bindi, M., Carozzi, M., Cavalli, D., Conant, R., Dorich, C.D., Doro, L., Ehrhardt, F., Farina, R., Ferrise, R., Fitton, N., Francaviglia, R., Grace, P., Iocola, I., Klumpp, K., Léonard, J., Martin, R., Massad, R.S., Recous, S., Seddaiu, G., Sharp, J., Smith, P., Smith, W.N., Soussana, J.-F., Bellocchi, G., 2017. Review and analysis of strengths and weaknesses of agro-ecosystem models for simulating C and N fluxes. Sci. Total Environ. 598, 445–470. https://doi.org/10.1016/j.scitotenv.2017.03.208.

Chambers, A., Lal, R., Paustian, K., 2016. Soil carbon sequestration potential of US croplands and grasslands: Implementing the 4 per ThoUSAnd Initiative. J. Soil Water Conserv. 71, 68A–74A. https://doi.org/10.2489/jswc.71.3.68A.

Deines, J.M., Wang, S., Lobell, D.B., 2019. Satellites reveal a small positive yield effect from conservation tillage across the US Corn Belt. Environ. Res. Lett. 14, 124038 https://doi.org/10.1088/1748-9326/ab503b.

Dold, C., Büyükcangaz, H., Rondinelli, W., Prueger, J.H., Sauer, T.J., Hatfield, J.L., 2017. Long-term carbon uptake of agro-ecosystems in the Midwest. Agric. For. Meteorol. 232, 128–140. https://doi.org/10.1016/j.agrformet.2016.07.012.

Drewniak, B., Song, J., Prell, J., Kotamarthi, V.R., Jacob, R., 2013. Modeling agriculture in the community land model. Geosci. Model Dev. 6, 495–515. https://doi.org/10.5194/gmd-6-495-2013.

Farquhar, G.D., von Caemmerer, S., Berry, J.A., 1980. A biochemical model of photosynthetic CO2 assimilation in leaves of C3 species. Planta. https://doi.org/10.1007/bf00386231.

Gilhespy, S.L., Anthony, S., Cardenas, L., Chadwick, D., del Prado, A., Li, C., Misselbrook, T., Rees, R.M., Salas, W., Sanz-Cobena, A., Smith, P., Tilston, E.L., Topp, C.F.E., Vetter, S., Yeluripati, J.B., 2014. First 20 years of DNDC (DeNitrification DeComposition): Model evolution. Ecol. Modell. 292, 51–62. https://doi.org/10.1016/j.ecolmodel.2014.09.004.

Grant, R.F., Lin, S., Hernandez-Ramirez, G., 2020. Modelling nitrification inhibitor effects on N2O emissions after fall-and spring-Applied slurry by reducing nitrifier NH4+ oxidation rate. Biogeosciences 17, 2021–2039. https://doi.org/10.5194/bg-17-2021-2020.

Grant, R., 1997. Changes in Soil organic matter under different tillage and rotation: mathematical modeling in ecosys. Soil Sci. Soc. Am. J. https://doi.org/10.2136/sssaj1997.03615995006100040023x.

Grant, R., Arkebauer, T., Dobermann, A., Hubbard, K., Schimelfenig, T., Suyker, A., Verma, S., Walters, D., 2007. Net biome productivity of irrigated and rainfed maize-soybean rotations: modeling vs. measurements. Agron. J. https://doi.org/10.2134/agronj2006.0308.

Grant, R., Barr, A., Black, T., Margolis, H., McCaughey, J., Trofymow, J., 2010. Net ecosystem productivity of temperate and boreal forests after clearcutting–a Fluxnet-Canada measurement and modelling synthesis. Tellus B. https://doi.org/10.3402/tellusb.v62i5.16588.

Grant, R.F., 2014. Nitrogen mineralization drives the response of forest productivity to soil warming: modelling in ecosys vs. measurements from the Harvard soil heating experiment. Ecol. Modell. 288, 38–46. https://doi.org/10.1016/j.ecolmodel.2014.05.015.

Grant, R.F., 2013. Modelling changes in nitrogen cycling to sustain increases in forest productivity under elevated atmospheric $CO_2$ and contrasting site conditions. Biogeosciences. https://doi.org/10.5194/bg-10-7703-2013.

Grant, R.F., 2004. Modeling topographic effects on net ecosystem productivity of boreal black spruce forests. Tree Physiol. 24, 1–18. https://doi.org/10.1093/treephys/24.1.1.

Grant, R.F., 2001. A review of the Canadian ecosystem model — ecosys. Model. Carbon Nitrogen Dyn. Soil Manage. https://doi.org/10.1201/9781420032635.ch6.

Grant, R.F., 1998. Simulation in ecosys of root growth response to contrasting soil water and nitrogen. Ecol. Modell. 107, 237–264. https://doi.org/10.1016/S0304-3800(97)00221-4.

Grant, R.F., 1995. Salinity, water use and yield of maize: testing of the mathematical model ecosys. Plant Soil. https://doi.org/10.1007/bf00011333.

Grant, R.F., 1989a. Test of a simple biochemical model for photosynthesis of maize and soybean leaves. Agric. For. Meteorol. 48, 59–74. https://doi.org/10.1016/0168-1923(89)90007-5.

Grant, R.F., 1989b. Simulation of carbon assimilation and partitioning in maize. Agron. J. https://doi.org/10.2134/agronj1989.00021962008100040004x.

Grant, R.F., 1989c. Simulation of maize phenology. Agron. J. https://doi.org/10.2134/agronj1989.00021962008100030011x.

Grant, R.F., Baldocchi, D.D., Ma, S., 2012. Ecological controls on net ecosystem productivity of a seasonally dry annual grassland under current and future climates: modelling with ecosys. Agric. For. Meteorol. 152, 189–200. https://doi.org/10.1016/j.agrformet.2011.09.012.

Grant, R.F., Flanagan, L.B., 2007. Modeling stomatal and nonstomatal effects of water deficits on CO2 fixation in a semiarid grassland. J. Geophys. Res. Biogeosci. 112 https://doi.org/10.1029/2006JG000302.

Grant, R.F., Goulden, M.L., Wofsy, S.C., Berry, J.A., 2001. Carbon and energy exchange by a black spruce-moss ecosystem under changing climate: Testing the mathematical model ecosys with data from the BOREAS experiment. J. Geophys. Res. Atmos. 106, 33605–33621. https://doi.org/10.1029/2001JD900064.

Grant, R.F., Kimball, B.A., Conley, M.M., White, J.W., Wall, G.W., Ottman, M.J., 2011. Controlled warming effects on wheat growth and yield: field measurements and modeling. Agron. J. https://doi.org/10.2134/agronj2011.0158.

Grant, R.F., Neftel, A., Calanca, P., 2016. Ecological controls on N2O emission in surface litter and near-surface soil of a managed grassland: modelling and measurements. Biogeosciences 13, 3549–3571. https://doi.org/10.5194/bg-13-3549-2016.

Grant, R.F., Pattey, E., 2008. Temperature sensitivity of N 2 O emissions from fertilized agricultural soils: mathematical modeling in ecosys. Global Biogeochem. Cycles 22. https://doi.org/10.1029/2008GB003273 n/a-n/a.

Grant, R.F., Pattey, E., 2003. Modelling variability in N2O emissions from fertilized agricultural fields. Soil Biol. Biochem. 35, 225–243. https://doi.org/10.1016/S0038-0717(02)00256-0.

Grant, R.F., Pattey, E., Goddard, T.W., Kryzanowski, L.M., Puurveen, H., 2006. Modeling the effects of fertilizer application rate on nitrous oxide emissions. Soil Sci. Soc. Am. J. 70, 235–248. https://doi.org/10.2136/sssaj2005.0104.

Grant, R.F., Peters, D.B., Larson, E.M., Huck, M.G., 1989. Simulation of canopy photosynthesis in maize and soybean. Agric. For. Meteorol. 48, 75–92. https://doi.org/10.1016/0168-1923(89)90008-7.

Grant, R.F., Rochette, P., 1994. Soil microbial respiration at different water potentials and temperatures: theory and mathematical modeling. Soil Sci. Soc. Am. J. https://doi.org/10.2136/sssaj1994.03615995005800060015x.

Grant, R.F., Rochette, P., Desjardins, R.L., 1993. Energy exchange and water use efficiency of field crops: validation of a simulation model. Agron. J. https://doi.org/10.2134/agronj1993.00021962008500040025x.


Grant, R.F., Goulden, M.L., Wofsy, S.C., Berry, J.A., 2001. Carbon and energy exchange by a black spruce-moss ecosystem under changing climate: Testing the mathematical model ecosys with data from the BOREAS experiment. J. Geophys. Res. Atmos. 106, 33605–33621. https://doi.org/10.1029/2001JD900064.


Grant, R., Juma, N.G., Robertson, J.A., Izaurralde, R.C., McGill, W.B., 2001b. Long-term changes in soil carbon under different fertilizer, manure, and rotation: testing the mathematical model ecosys with data from the breton plots. Soil Sci. Soc. Am. J., NATO ASI Series I3865, 205–214. https://doi.org/10.2136/sssaj2001.651205x.

Grant, R., Juma, N., Robertson, J., Izaurralde, R., McGill, W., 2001c. Long-term changes in soil carbon under different fertilizer, manure, and rotation. Soil Sci. Soc. Am. J. https://doi.org/10.2136/sssaj2001.1872a.

Grant, R., Mekonnen, Z., Riley, W., 2019. Modeling climate change impacts on an arctic polygonal Tundra: 1. Rates of permafrost thaw depend on changes in vegetation and drainage. J. Geophys. Res. Biogeosci. 124, 1308–1322. https://doi.org/10.1029/2018JG004644.

Grant, R.F., Wall, G.W., Kimball, B.A., Frumau, K.F.A., Pinter, P.J., Hunsaker, D.J., Lamorte, R.L., 1999. Crop water relations under different CO2 and irrigation: testing of ecosys with the free air CO2 enrichment (FACE) experiment. Agric. For. Meteorol. 95, 27–51. https://doi.org/10.1016/S0168-1923(99)00017-9.

Grant, R., Zhang, Y., Yuan, F., Wang, S., Hanson, P., Gaumont-Guay, D., Chen, J., Black, T., Barr, A., Baldocchi, D., Arain, A., 2006. Intercomparison of techniques to model water stress effects on CO2 and energy exchange in temperate and boreal deciduous forests. Ecol. Modell. https://doi.org/10.1016/j.ecolmodel.2006.02.035.

Griffis, T.J., Sargent, S.D., Baker, J.M., Lee, X., Tanner, B.D., Greene, J., Swiatek, E., Billmark, K., 2008. Direct measurement of biosphere-atmosphere isotopic CO2exchange using the eddy covariance technique. J. Geophys. Res. https://doi.org/10.1029/2007jd009297.

Gurung, R.B., Ogle, S.M., Breidt, F.J., Williams, S.A., Parton, W.J., 2020. Bayesian calibration of the DayCent ecosystem model to simulate soil organic carbon dynamics and reduce model uncertainty. Geoderma 376, 114529. https://doi.org/10.1016/j.geoderma.2020.114529.

Hernandez-Ramirez, G., Hatfield, J.L., Parkin, T.B., Sauer, T.J., Prueger, J.H., 2011. Carbon dioxide fluxes in corn–soybean rotation in the midwestern U.S.: inter- and intra-annual variations, and biophysical controls. Agric. For. Meteorol. https://doi.org/10.1016/j.agrformet.2011.07.017.

Huang, Y., Yu, Y., Zhang, W., Sun, W., Liu, S., Jiang, J., Wu, J., Yu, W., Wang, Y., Yang, Z., 2009. Agro-C: a biogeophysical model for simulating the carbon budget of agroecosystems. Agric. For. Meteorol. 149, 106–129. https://doi.org/10.1016/j.agrformet.2008.07.013.

Hutchinson, J.J., Campbell, C.A., Desjardins, R.L., 2007. Some perspectives on carbon sequestration in agriculture. Agric. For. Meteorol. 142, 288–302. https://doi.org/10.1016/j.agrformet.2006.03.030.

Jandl, R., Rodeghiero, M., Martinez, C., Cotrufo, M.F., Bampa, F., van Wesemael, B., Harrison, R.B., Guerrini, I.A., Richter Jr., D.D., Rustad, L., Lorenz, K., Chabbi, A., Miglietta, F., 2014. Current status, uncertainty and future needs in soil organic carbon monitoring. Sci. Total Environ. 468–469. https://doi.org/10.1016/j.scitotenv.2013.08.026, 376–383.

Jarecki, M.K., Lal, R., 2003. Crop Management for Soil Carbon Sequestration. Crit. Rev. Plant Sci. https://doi.org/10.1080/713608318.

Jiang, C., Guan, K., Wu, G., Peng, B., Wang, S., 2021. A daily, 250 m and real-time gross primary productivity product (2000–present) covering the contiguous United States. Earth Syst. Sci. Data 13, 281–298. https://doi.org/10.5194/essd-13-281-2021.

Jin, Z., Zhuang, Q., Wang, J., Archontoulis, S.V., Zobel, Z., Kotamarthi, V.R., 2017. The combined and separate impacts of climate extremes on the current and future US rainfed maize and soybean production under elevated CO2. Glob. Chang. Biol. 23, 2687–2704. https://doi.org/10.1111/gcb.13617.

Kimble, J.M., Follett, R.F., Vernon Cole, C., 1998. The Potential of U.S. Cropland to Sequester Carbon and Mitigate the Greenhouse Effect. CRC Press.

Kimm, H., Guan, K., Gentine, P., Wu, J., Bernacchi, C.J., Sulman, B.N., Griffis, T.J., Lin, C., 2020. Redefining droughts for the U.S. Corn Belt: the dominant role of atmospheric vapor pressure deficit over soil moisture in regulating stomatal behavior of Maize and Soybean. Agric. For. Meteorol. 287, 107930 https://doi.org/10.1016/j.agrformet.2020.107930.

Kuppel, S., Peylin, P., Chevallier, F., Bacour, C., Maignan, F., Richardson, A.D., 2012. Constraining a global ecosystem model with multi-site eddy-covariance data. https://doi.org/10.5194/bg-9-3757-2012.

Lal, R., 2011. Sequestering carbon in soils of agro-ecosystems. Food Policy. https://doi.org/10.1016/j.foodpol.2010.12.001.

Lal, R., Follett, R.F., Stewart, B.A., Kimble, J.M., 2007. Soil carbon sequestration to mitigate climate change and advance food security. Soil Sci. 172.

Lal, R., 2004. Soil carbon sequestration impacts on global climate change and food security. Science 304, 1623–1627. https://doi.org/10.1126/science.1097396.

Lal, R., 2002. Soil carbon dynamics in cropland and rangeland. Environ. Pollut. 116, 353–362. https://doi.org/10.1016/s0269-7491(01)00211-1.

Lal, R., 2001. World cropland soils as a source or sink for atmospheric carbon. Adv. Agronomy. https://doi.org/10.1016/s0065-2113(01)71014-0.

Li, C., Frolking, S., Crocker, G.J., Grace, P.R., Klír, J., Körchens, M., Poulton, P.R., 1997. Simulating trends in soil organic carbon in long-term experiments using the DNDC model. Geoderma 81, 45–60. https://doi.org/10.1016/S0016-7061(97)00080-3.

Liu, X., Chen, F., Barlage, M., Zhou, G., Niyogi, D., 2016. Noah-MP-Crop: Introducing dynamic crop growth in the Noah-MP land surface model. J. Geophys. Res. 121, 953-972. https://doi.org/10.1002/2016JD025597.

Liu, Y., Yu, Z., Chen, J., Zhang, F., Doluschitz, R., Axmacher, J.C., 2006. Changes of soil organic carbon in an intensively cultivated agricultural region: a denitrification-decomposition (DNDC) modelling approach. Sci. Total Environ. 372, 203–214. https://doi.org/10.1016/j.scitotenv.2006.09.022.

Li, Y., Guan, K., Schnitkey, G.D., DeLucia, E., Peng, B., 2019. Excessive rainfall leads to maize yield loss of a comparable magnitude to extreme drought in the United States. Glob. Chang. Biol. 25, 2325–2337. https://doi.org/10.1111/gcb.14628.

Lobell, D.B., Roberts, M.J., Schlenker, W., Braun, N., Little, B.B., Rejesus, R.M., Hammer, G.L., 2014. Greater sensitivity to drought accompanies maize yield increase in the U.S. Midwest. Science 344, 516–519. https://doi.org/10.1126/science.1251423.

Mäkelä, A., Pulkkinen, M., Kolari, P., Lagergren, F., Berbigier, P., Lindroth, A., Loustau, D., Nikinmaa, E., Vesala, T., Hari, P., 2007. Developing an empirical model of stand GPP with the LUE approach: analysis of eddy covariance data at five contrasting conifer sites in Europe. Glob. Chang. Biol. 0 https://doi.org/10.1111/j.1365-2486.2007.01463.x, 071124112207003–???

Meena, R.S., Kumar, S., Yadav, G.S., 2020. Soil carbon sequestration in crop production. In: Meena, R.S. (Ed.), Nutrient Dynamics for Sustainable Crop Production. Springer, Singapore, Singapore, pp. 1–39. https://doi.org/10.1007/978-981-13-8660-2_1.

Mehra, P., Baker, J., Sojka, R.E., Bolan, N., Desbiolles, J., Kirkham, M.B., Ross, C., Gupta, R., 2018. A review of tillage practices and their potential to impact the soil carbon dynamics. Advances in Agronomy. Elsevier Inc., pp. 185–230. https://doi.org/10.1016/bs.agron.2018.03.002

Mekonnen, Z.A., Grant, R.F., Schwalm, C., 2017. Carbon sources and sinks of North America as affected by major drought events during the past 30 years. Agric. For. Meteorol. 244–245, 42–56. https://doi.org/10.1016/j.agrformet.2017.05.006.

Meyers, T., 2004. An assessment of storage terms in the surface energy balance of maize and soybean. Agric. For. Meteorol.

Mezbahuddin, M., Grant, R.F., Flanagan, L.B., 2017. Coupled eco-hydrology and biogeochemistry algorithms enable the simulation of water table depth effects on boreal peatland net CO2 exchange. Biogeosciences 14, 5507–5531. https://doi.org/10.5194/bg-14-5507-2017.

Mezbahuddin, S., Spiess, D., Hildebrand, D., Kryzanowski, L., Itenfisu, D., Goddard, T., Iqbal, J., Grant, R., 2020. Assessing effects of agronomic nitrogen management on crop nitrogen use and nitrogen losses in the western canadian prairies. Front. Sustainable Food Syst. https://doi.org/10.3389/fsufs.2020.512292.

Osborne, B., Saunders, M., Walmsley, D., Jones, M., Smith, P., 2010. Key questions and uncertainties associated with the assessment of the cropland greenhouse gas balance. Agric. Ecosyst. Environ. 139, 293–301. https://doi.org/10.1016/j.agee.2010.05.009.

Peng, B., Guan, K., Chen, M., Lawrence, D.M., Pokhrel, Y., Suyker, A., Arkebauer, T., Lu, Y., 2018. Improving maize growth processes in the community land model: implementation and evaluation. Agric. For. Meteorol. 250-251, 64–89. https://doi.org/10.1016/j.agrformet.2017.11.012.

Peng, B., Guan, K., Tang, J., Ainsworth, E.A., Asseng, S., Bernacchi, C.J., Cooper, M., Delucia, E.H., Elliott, J.W., Ewert, F., Grant, R.F., Gustafson, D.I., Hammer, G.L., Jin, Z., Jones, J.W., Kimm, H., Lawrence, D.M., Li, Y., Lombardozzi, D.L., Marshall-Colon, A., Messina, C.D., Ort, D.R., Schnable, J.C., Vallejos, C.E., Wu, A., Yin, X.,

Zhou, W., 2020. Towards a multiscale crop modelling framework for climate change adaptation assessment. Nat. Plants 6, 338–348. https://doi.org/10.1038/s41477-020-0625-3.
Poeplau, C., Don, A., 2015. Carbon sequestration in agricultural soils via cultivation of cover crops – a meta-analysis. Agric. Ecosyst. Environ. 200, 33–41. https://doi.org/10.1016/j.agee.2014.10.024.
Salmon, Y., Lintunen, A., Dayet, A., Chan, T., Dewar, R., Vesala, T., Hölttä, T., 2020. Leaf carbon and water status control stomatal and nonstomatal limitations of photosynthesis in trees. New Phytol. 226, 690–703. https://doi.org/10.1111/nph.16436.
Seifert, C.A., Azzari, G., Lobell, D.B., 2019. Corrigendum: satellite detection of cover crops and their effects on crop yield in the Midwestern United States (2018 Environ. Res. Let. 13 064033). Environ. Res. Lett. 14, 039501 https://doi.org/10.1088/1748-9326/aaf933.
Schrumpf, M., Schulze, E.D., Kaiser, K., Schumacher, J., 2011. How accurately can soil organic carbon stocks and stock changes be quantified by soil inventories? https://doi.org/10.5194/bg-8-1193-2011.
Shekoofa, A., Safikhan, S., Snider, J.L., Raper, T.B., Bourland, F.M., 2021. Variation in stomatal conductance responses of cotton cultivars to high vapour pressure deficit under controlled and rainfed environments. J. Agron. Crop Sci. 207, 332–343. https://doi.org/10.1111/jac.12440.
Shirato, Y., 2005. Testing the suitability of the DNDC model for simulating long-term soil organic carbon dynamics in Japanese paddy soils. Soil Sci. Plant Nutr. 51, 183–192. https://doi.org/10.1111/j.1747-0765.2005.tb00022.x.
Stehfest, E., Heistermann, M., Priess, J.A., Ojima, D.S., Alcamo, J., 2007. Simulation of global crop production with the ecosystem model DayCent. Ecol. Modell. 209, 203–219. https://doi.org/10.1016/j.ecolmodel.2007.06.028.
Suyker, A.E., Verma, S.B., 2012. Gross primary production and ecosystem respiration of irrigated and rainfed maize–soybean cropping systems over 8 years. Agric. For. Meteorol. https://doi.org/10.1016/j.agrformet.2012.05.021.
Suyker, A.E., Verma, S.B., Burba, G.G., Arkebauer, T.J., 2005. Gross primary production and ecosystem respiration of irrigated maize and irrigated soybean during a growing season. Agric. For. Meteorol. https://doi.org/10.1016/j.agrformet.2005.05.007.
Tarantola, A., 2013. Inverse Problem Theory: Methods for Data Fitting and Model Parameter Estimation. Elsevier.
USDA, 2021. USDA National Agricultural Statistics Service National 2020 Cultivated Layer. USDA-NASS, Washington, DC. Available at. https://www.nass.usda.gov/Research_and_Science/Cropland/Release/index.php (accessed May 2021).
USDA, 2020. Crop Production 2019 Summary. https://www.nass.usda.gov/Publications/Todays_Reports/reports/cropan20.pdf.
USDA, 2019. Fertilizer Use and Price. https://www.ers.usda.gov/data-products/fertilizer-use-and-price/.
VandenBygaart, A.J., Angers, D.A., 2006. Towards accurate measurements of soil organic carbon stock change in agroecosystems. Can. J. Soil Sci. 86, 465–471. https://doi.org/10.4141/S05-106.
van Wesemael, B., Paustian, K., Meersmans, J., Goidts, E., Barancikova, G., Easter, M., 2010. Agricultural management explains historic changes in regional soil carbon stocks. Proc. Natl. Acad. Sci. USA 107, 14926–14930. https://doi.org/10.1073/pnas.1002592107.
Verma, S.B., Dobermann, A., Cassman, K.G., Walters, D.T., Knops, J.M., Arkebauer, T.J., Suyker, A.E., Burba, G.G., Amos, B., Yang, H., Ginting, D., Hubbard, K.G., Gitelson, A.A., Walter-Shea, E.A., 2005. Annual carbon dioxide exchange in irrigated and rainfed maize-based agroecosystems. Agric. For. Meteorol. 131, 77–96. https://doi.org/10.1016/j.agrformet.2005.05.003.
Van den Hoof, C., Hanert, E., Vidale, P.L., 2011. Simulating dynamic crop growth with an adapted land surface model – JULES-SUCROS: model development and validation. Agric. For. Meteorol. 151, 137–153. https://doi.org/10.1016/j.agrformet.2010.09.011.
Vogel, F.A., 2018. Understanding USDA Crop Forecasts: March 1999 (Classic Reprint). Forgotten Books.
Wang, S., Garcia, M., Ibrom, A., Bauer-Gottwein, P., 2020. Temporal interpolation of land surface fluxes derived from remote sensing – results with an unmanned aerial system. Hydrol. Earth Syst. Sci. 24, 3643–3661. https://doi.org/10.5194/hess-24-3643-2020.
Wattenbach, M., Sus, O., Vuichard, N., Lehuger, S., Gottschalk, P., Li, L., Leip, A., Williams, M., Tomelleri, E., Kutsch, W.L., Buchmann, N., Eugster, W., Dietiker, D., Aubinet, M., Ceschia, E., Béziat, P., Grünwald, T., Hastings, A., Osborne, B., Ciais, P., Cellier, P., Smith, P., 2010. The carbon balance of European croplands: a cross-site comparison of simulation models. Agric. Ecosyst. Environ. 139, 419–453. https://doi.org/10.1016/j.agee.2010.08.004.
West, T.O., Brandt, C.C., Baskaran, L.M., Hellwinckel, C.M., Mueller, R., Bernacchi, C.J., Bandaru, V., Yang, B., Wilson, B.S., Marland, G., Nelson, R.G., De la Torre Ugarte, D. G., Post, W.M., 2010. Cropland carbon fluxes in the United States: increasing geospatial resolution of inventory-based carbon accounting. Ecol. Appl. 20, 1074–1086. https://doi.org/10.1890/08-2352.1.
West, T.O., Brandt, C.C., Wilson, B.S., Hellwinckel, C.M., Tyler, D.D., Marland, G., De La Torre Ugarte, D.G., Larson, J.A., Nelson, R.G., 2008. Estimating regional changes in soil carbon with high spatial resolution. Soil Sci. Soc. Am. J. 72, 285–294. https://doi.org/10.2136/sssaj2007.0113.
West, T.O., Brown, M.E., Duren, R.M., Ogle, S.M., Moss, R.H., 2013. Definition, capabilities and components of a terrestrial carbon monitoring system. Carbon Manage. https://doi.org/10.4155/cmt.13.36.
West, T.O., Marland, G., 2002. A synthesis of carbon sequestration, carbon emissions, and net carbon flux in agriculture: comparing tillage practices in the United States. Agric. Ecosyst. Environ. 91, 217–232. https://doi.org/10.1016/S0167-8809(01)00233-X.
Xue, F., Tong, L., Liu, W., Cao, H., Song, L., Ji, S., Ding, R., 2021. Stomatal conductance of tomato leaves is regulated by both abscisic acid and leaf water potential under combined water and salt stress 1–9. https://doi.org/10.1111/ppl.13441.
Yokohata, T., Kinoshita, T., Sakurai, G., Pokhrel, Y., Ito, A., Okada, M., Satoh, Y., Kato, E., Nitta, T., Fujimori, S., Felfelani, F., Masaki, Y., Iizumi, T., Nishimori, M., Hanasaki, N., Takahashi, K., Yamagata, Y., Emori, S., 2020. MIROC-INTEG-LAND version 1: a global biogeochemical land surface model with human water management, crop growth, and land-use change. Geosci. Model. Dev. 13, 4713–4747. https://doi.org/10.5194/gmd-13-4713-2020.
Zhang, X., Izaurralde, R.C., Manowitz, D.H., Sahajpal, R., West, T.O., Thomson, A.M., Xu, M., Zhao, K., LeDuc, S.D., Williams, J.R., 2015. Regional scale cropland carbon budgets: evaluating a geospatial agricultural modeling system using inventory data. Environ. Model. Softw. 63, 199–216. https://doi.org/10.1016/j.envsoft.2014.10.005.
Zhang, J., Guan, K., Peng, B., Jiang, C., Zhou, W., Yang, Y., Pan, M., Franz, T., Heeren, D., Rudnick, D., Abimbola, O., Kimm, H., Caylor, K., Good, S., Khanna, M., Gates, J., Cai, Y., 2021. Challenges and opportunities in precision irrigation decision-support systems for center pivots. Environ. Res. Lett. 16 (5), 053003 https://doi.org/10.1088/1748-9326/abe436.
Zhang, Y., Gurung, R., Marx, E., Williams, S., Ogle, S.M., Paustian, K., 2020. DayCent model predictions of NPP and grain yields for agricultural lands in the contiguous U. S. J. Geophys. Res. Biogeosci. https://doi.org/10.1029/2020JG005750.
Zhou, W., Guan, K., Peng, B., Shi, J., Jiang, C., Wardlow, B., Pan, M., Kimball, J.S., Franz, T.E., Gentine, P., He, M., Zhang, J., 2020. Connections between the hydrological cycle and crop yield in the rainfed U.S. Corn Belt. J. Hydrol. 590, 125398 https://doi.org/10.1016/j.jhydrol.2020.125398.